SIAM J. MATH. ANAL.
Vol. 52, No. 1, pp. 1–41

THE ORBITAL STABILITY OF ELLIPTIC SOLUTIONS OF THE FOCUSING NONLINEAR SCHRÖDINGER EQUATION*

BERNARD DECONINCK† AND JEREMY UPSAL†

Abstract. We examine the stability of the elliptic solutions of the focusing nonlinear Schrödinger equation (NLS) with respect to subharmonic perturbations. Using the integrability of NLS, we discuss the spectral stability of the elliptic solutions, establishing that solutions of smaller amplitude are stable with respect to larger classes of perturbations. We show that spectrally stable solutions are orbitally stable by constructing a Lyapunov functional using higher-order conserved quantities of NLS.

Key words. stability, NLS, elliptic, focusing, subharmonic, integrability

AMS subject classifications. 37K45, 35Q55, 33E05

DOI. 10.1137/19M1240757

1. Introduction.

The focusing, one-dimensional, cubic nonlinear Schrödinger equation (NLS),

$$i\Psi_t + \frac{1}{2}\Psi_{xx} + \Psi\,|\Psi|^2 = 0, \tag{1}$$

is a universal model for a variety of physical phenomena [10, 23, 29, 36, 39, 44]. In 1972, Zakharov and Shabat [45] found its Lax pair and the explicit expression for the one-soliton solution. The orbital stability of the soliton was first proved in 1982 by Cazenave and Lions [9] and later by Weinstein [41] using Lyapunov techniques, as used here. Even with such a rich history, a full stability analysis in the periodic setting has not been completed. The simplest periodic solutions are the genus-one or elliptic solutions (section 2). Rowlands [37] was the first to study their stability using perturbation methods. Since then, Gallay and Hărăguş have examined the stability of small-amplitude elliptic solutions [18] and proven orbital stability with respect to perturbations of the same period as the underlying solution [19] (i.e., coperiodic perturbations). Gustafson, Le Coz, and Tsai [24] establish instability for the elliptic solutions with respect to sufficiently large perturbations. The analysis of spectral instability with respect to perturbations of an integer multiple of the period (i.e., subharmonic perturbations) was completed in [16].

In this work we build upon the results in [16] to examine the stability of elliptic solutions of arbitrary amplitude. Only classical solutions of (1) and classical perturbations of those solutions are considered in this paper. An outline of the steps follows and the conclusions obtained are given below.

1. Spectral stability is considered in section 3. This is motivated by considering the simpler case of the well-known Stokes waves in section 3.2. For these solutions, all operators involved have constant coefficients, and all calculations are explicit. We get to the spectrum of the operator obtained by linearizing

---

*Received by the editors January 29, 2019; accepted for publication (in revised form) October 21, 2019; published electronically January 2, 2020.
https://doi.org/10.1137/19M1240757
Funding: The work of the first author was supported by National Science Foundation grant DMS-1522677.
†Department of Applied Mathematics, University of Washington, Seattle, WA 98195 (bernard@amath.washington.edu, jupsal@u.washington.edu).

about a solution through its connection with the *Lax spectrum*. To this end, we introduce the Lax pair and its spectrum in section 3.3. The results in section 3.3.1 are from [16], while the results in section 3.3.2 and all subsequent sections are new. Section 3.4 contains our main spectral stability result: solutions are spectrally stable with respect to subharmonic perturbations if the solution parameters meet a given sufficiency condition (Theorem 4). This condition is shown to be necessary in most cases and is discussed in Appendix C. In essence, Theorem 4 establishes that solutions of "smaller amplitude" are spectrally stable with respect to a larger class of subharmonic perturbations, i.e., subharmonic perturbations of larger period. The notion of "smaller amplitude" is made more precise in section 3.4.

2. In section 4, we examine how instabilities depend on the parameters of the solution. The orbital stability results of section 5 rely crucialy on understanding the spectrum for stable compared to unstable solutions. Thus we carefully examine the transition from stable to unstable dynamics as solution parameters are changed.
3. Finally, in section 5 we use a Lyapunov method [22, 27, 34] to prove (nonlinear) orbital stability in the cases where spectral stability holds. Our main result is found at the end of the section: we establish the orbital stability of almost all solutions that are spectrally stable. The only solutions for which such a result eludes us are those whose solution parameters are on the boundary of the parameter regions specifying with respect to which subharmonic perturbations the solutions are spectrally stable.

This paper is part of an ongoing research program of analyzing the stability of periodic solutions of integrable equations [5, 6, 12, 14, 15, 16, 35]. The present work is the first in the program to establish a nonlinear stability result for periodic solutions for which the underlying Lax pair is not self-adjoint.

2. Elliptic solutions of focusing NLS. In this paper we study solutions of (1) whose only change in time is through a constant phase-change. Such solutions are stationary solutions of

$$i\psi_t + \omega\psi + \frac{1}{2}\psi_{xx} + \psi\,|\psi|^2 = 0, \tag{2}$$

found by defining $\Psi(x,t) = e^{-i\omega t}\psi(x,t)$. Time-independent solutions to (2) satisfy

$$\omega\phi + \frac{1}{2}\phi_{xx} + \phi\,|\phi|^2 = 0 \tag{3}$$

and are expressed in terms of elliptic functions as

$$\Psi = e^{-i\omega t}\phi(x) = R(x)e^{i\theta(x)}e^{-i\omega t} \tag{4}$$

with

$$R^2(x) = b - k^2\,\mathrm{sn}^2(x,k), \qquad \omega = \frac{1}{2}\left(1 + k^2 - 3b\right), \tag{5a}$$

$$\theta(x) = c\int_0^x \frac{1}{R^2(y)}\,\mathrm{d}y, \qquad c^2 = b(1-b)(b-k^2), \tag{5b}$$

where $\mathrm{sn}(x,k)$ is the Jacobi elliptic sn function with elliptic modulus k [1, Chapter 22]. The parameters b and k are constrained by

$$0 \le k < 1, \qquad k^2 \le b \le 1; \tag{6}$$

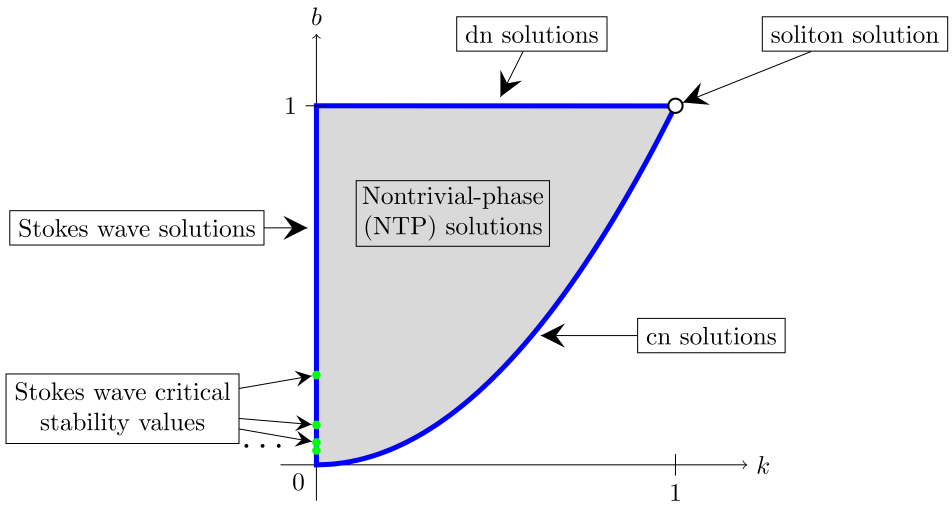

Fig. 1. *The parameter space for the elliptic solutions* (4) *with solution regions labeled. The first four Stokes wave stability bounds are plotted in green dots on the line $k = 0$, at which $b = 1/P^2$ for $P \in \{1, 2, 3, 4\}$* (28).

see Figure 1. The solutions formally limit to the soliton as $k \to 1$, which is omitted from our studies. When $k = 0$ and $b \neq 0$, (4) reduces to a so-called Stokes wave (section 3.2). The boundary values, $b = k^2$ and $b = 1$, are special cases. In both cases $c = 0$ so $\theta = 0$ and the solutions are said to have trivial phase. When $c \neq 0$, the solutions have nontrivial phase (NTP). We call $\phi(x) = k\,\mathrm{cn}(x, k)$ and $\phi(x) = \mathrm{dn}(x, k)$ the cn and dn solutions corresponding to $b = k^2$ and $b = 1$, respectively. Here $\mathrm{cn}(x, k)$ and $\mathrm{dn}(x, k)$ are the Jacobi elliptic cn and dn functions with elliptic modulus k [1, Chapter 22]. The trivial-phase solutions are periodic, with periods $4K(k)$ and $2K(k)$ for the cn and dn solutions, respectively, where

$$K(k) := \int_0^{\pi/2} \frac{\mathrm{d}y}{\sqrt{1 - k^2 \sin^2(y)}}, \tag{7}$$

the complete elliptic integral of the first kind [1, Chapter 19].

Remark 1. The NTP solutions are typically quasi-periodic but only the x-periodic amplitude $R^2(x)$ appears in our analysis. Therefore, unless otherwise stated, any mention of the periodicity of the solutions is in reference to the period of the amplitude which is $T(k) = 2K(k)$ for all solutions.

The elliptic solutions can be written in terms of Weierstrass elliptic functions via

$$\wp(z + \omega_3; g_2, g_3) - e_3 = \left(\frac{K(k)k}{\omega_1}\right)^2 \mathrm{sn}^2\left(\frac{K(k)z}{\omega_1}\right), \tag{8}$$

where $\wp(z; g_2, g_3)$ is the Weierstrass elliptic $\wp$ function [1, Chapter 23] with lattice invariants g_2, g_3 and ω_1 and ω_3 are the half-periods of the Weierstrass lattice. Last, e_1, e_2, and e_3 are the zeros of the polynomial $4t^3 - g_2 t - g_3$, and

(9a)
$$e_1 = \frac{1}{3}(2-k^2), \qquad e_2 = \frac{1}{3}(2k^2-1), \qquad e_3 = -\frac{1}{3}(1+k^2),$$
(9b)
$$g_2 = \frac{4}{3}(1-k^2+k^4), \qquad g_3 = \frac{4}{27}(2-3k^2-3k^4+2k^6),$$
(9c)
$$\omega_1 = \int_{e_1}^{\infty} \frac{\mathrm{d}z}{\sqrt{4z^3-g_2z-g_3}} = K(k), \quad \omega_3 = \int_{-e_3}^{\infty} \frac{\mathrm{d}z}{\sqrt{4z^3-g_2z-g_3}} = iK\left(\sqrt{1-k^2}\right).$$

The Weierstrass form of the elliptic solutions is explained in more detail in [11, section 3.1.3].

3. Spectral stability. Spectral stability of elliptic solutions is examined by considering

$$\Psi(x,t) = e^{-i\omega t}e^{i\theta(x)}\left(R(x)+\epsilon u(x,t)+\epsilon i v(x,t)\right)+\mathcal{O}\left(\epsilon^2\right), \tag{10}$$

where ϵ is a small parameter and u and v are real-valued functions of x and t. Substituting this into (1) and keeping only first-order in ϵ terms gives an autonomous ODE in t. Separating variables $(u(x,t),v(x,t)) = e^{\lambda t}(U(x),V(x))$ results in the spectral problem

$$\lambda\begin{pmatrix}U\\V\end{pmatrix} = \begin{pmatrix}-S & \mathcal{L}_-\\ -\mathcal{L}_+ & -S\end{pmatrix}\begin{pmatrix}U\\V\end{pmatrix} = J\begin{pmatrix}\mathcal{L}_+ & S\\ -S & \mathcal{L}_-\end{pmatrix}\begin{pmatrix}U\\V\end{pmatrix} = J\mathscr{L}\begin{pmatrix}U\\V\end{pmatrix} = \mathcal{L}\begin{pmatrix}U\\V\end{pmatrix}, \tag{11}$$

where

$$\mathcal{L} = J\mathscr{L}, \tag{12}$$

and

$$\begin{aligned}\mathcal{L}_- &= -\frac{1}{2}\partial_x^2 - R^2(x) - \omega + \frac{c^2}{2R^4(x)},\\ \mathcal{L}_+ &= -\frac{1}{2}\partial_x^2 - 3R^2(x) - \omega + \frac{c^2}{2R^4(x)},\\ S &= \frac{c}{R^2(x)}\partial_x - \frac{cR'(x)}{R^3(x)}.\end{aligned} \tag{13}$$

The stability spectrum is defined as

$$\sigma_{\mathcal{L}} = \left\{\lambda \in \mathbb{C} : U, V \in C_b^0(\mathbb{R})\right\}, \tag{14}$$

where $C_b^0(\mathbb{R})$ is the space of real-valued continuous functions, bounded on the closed real line. Due to the Hamiltonian symmetry of the spectrum [25], an elliptic solution is spectrally stable to perturbations in $C_b^0(\mathbb{R})$ if $\sigma_{\mathcal{L}} \subset i\mathbb{R}$.

3.1. Stability with respect to subharmonic perturbations. The elliptic solutions are not stable with respect to general bounded perturbations [16]. Therefore, we restrict to *subharmonic perturbations*. Subharmonic perturbations are those periodic perturbations whose period is an integer multiple of the fundamental period of a given elliptic solution. Since the operator $\mathcal{L}$ has periodic coefficients (13), the eigenfunctions of the spectral problem (11) may be decomposed using a Floquet–Bloch decomposition [13],

$$\begin{pmatrix} U(x) \\ V(x) \end{pmatrix} = e^{i\mu x} \begin{pmatrix} \hat{U}_\mu(x) \\ \hat{V}_\mu(x) \end{pmatrix}, \tag{15}$$

where $\hat{U}_\mu, \hat{V}_\mu$ are $T(k)$ periodic and $\mu \in [0, 2\pi/T(k))$.

Definition. *A* P-subharmonic perturbation *of a solution is a perturbation of integer multiple P times the period of the solution. A* 1*-subharmonic perturbation is called a* coperiodic perturbation.

For P-subharmonic perturbations,

$$\mu = m\frac{2\pi}{PT(k)}, \qquad m = 0, \ldots, P-1. \tag{16}$$

Note that μ may be defined in any interval of length $2\pi/T(k)$ so the $m = 1$ and $m = P - 1$ cases are connected via

$$\mu = -\frac{2\pi}{PT(k)} = (P-1)\frac{2\pi}{PT(k)} \qquad \mod 2\pi/T(k). \tag{17}$$

Using the Floquet–Bloch decomposition, $\mathcal{L} \mapsto \mathcal{L}_\mu$ with $\partial_x \mapsto \partial_x + i\mu$ in (11). We define the subharmonic stability spectrum with parameter μ,

$$\sigma_\mu = \left\{ \lambda \in \mathbb{C} : \hat{U}_\mu, \hat{V}_\mu \in L^2_{\text{per}}\left([-T(k)/2, T(k)/2]\right) \right\}, \tag{18}$$

where $L^2_{\text{per}}([-L/2, L/2])$ is the space of square-integrable functions with period L. The spectrum σ_μ consists of isolated eigenvalues of finite multiplicity.

3.2. Spectral stability of Stokes waves. We begin with the simplest case of (4). When $k = 0$, the solution is a Stokes wave solution of (1). The spectral stability of these solutions is straightforward to analyze, but the analysis is informative for understanding the general features of the stability of other solutions. We choose to work with the Stokes waves in this form to link them with the general elliptic solutions (4). The Stokes waves are given by

$$\Psi(x,t) = \sqrt{b}\; e^{ix\sqrt{1-b}}\; e^{-i(1-3b)t/2} \tag{19}$$

with parameter $b \in (0, 1]$. The spectral problem (11) becomes

$$\lambda \begin{pmatrix} U \\ V \end{pmatrix} = \begin{pmatrix} -\sqrt{1-b}\;\partial_x & -\frac{1}{2}\partial_x^2 \\ \frac{1}{2}\partial_x^2 + 2b & -\sqrt{1-b}\;\partial_x \end{pmatrix} \begin{pmatrix} U \\ V \end{pmatrix} = \mathcal{L}_S \begin{pmatrix} U \\ V \end{pmatrix}. \tag{20}$$

We consider the constant coefficients of $\mathcal{L}_S$ as π-periodic to match results below for the more general solutions of section 2, but the results for the Stokes waves are independent of this choice of period. Thus the eigenfunctions $(U, V)^T$ of (20) may be decomposed via a Floquet–Bloch decomposition (15)

$$\begin{pmatrix} U(x) \\ V(x) \end{pmatrix} = e^{i\mu x} \begin{pmatrix} \hat{U}(x) \\ \hat{V}(x) \end{pmatrix}, \tag{21}$$

where $\hat{U}$, $\hat{V}$ have period π and $\mu \in [0,2)$. Since (20) has constant coefficients, it suffices to consider each Fourier mode $(\hat{U}_n, \hat{V}_n)^T$ individually:

$$\lambda \begin{pmatrix} \hat{U}_n \\ \hat{V}_n \end{pmatrix} = \begin{pmatrix} -i\sqrt{1-b}\ (\mu+2n) & \frac{1}{2}(\mu+2n)^2 \\ 2b - \frac{1}{2}(\mu+2n)^2 & -i\sqrt{1-b}\ (\mu+2n) \end{pmatrix} \begin{pmatrix} \hat{U}_n \\ \hat{V}_n \end{pmatrix} = \hat{\mathcal{L}}_S^{(n,\mu)} \begin{pmatrix} \hat{U}_n \\ \hat{V}_n \end{pmatrix}, \tag{22}$$

where $n \in \mathbb{Z}$. The eigenvalues of $\hat{\mathcal{L}}_S^{(n,\mu)}$ are

$$\lambda_{\pm}^{(n,\mu)} = \frac{\mu+2n}{2}\left(-2i\sqrt{1-b} \pm \sqrt{4b-(\mu+2n)^2}\right). \tag{23}$$

These eigenvalues are imaginary if

$$\mu + 2n = 0 \quad \text{or} \quad b \leq (\mu+2n)^2/4. \tag{24}$$

The Stokes wave with amplitude b is spectrally stable with respect to bounded perturbations if (24) holds for all $n \in \mathbb{Z}$ and $\mu \in [0,2)$. For a given b, there exist μ and n such that (24) is not satisfied. Consequently, the Stokes waves are not spectrally stable with respect to general bounded perturbations. To examine stability with respect to special classes of perturbations, we consider special values of μ.

Equating $\mu = 0$ corresponds to perturbations with the same period as the solution. The spectral stability criterion (24) becomes $n = 0$ or $b \leq n^2$ which is satisfied for all n, independent of b, consistent with [16, 19]. For $\mu \neq 0$, the tightest bound on b from (24) is given by

$$b \leq \begin{cases} \mu^2/4, & \mu \in (0,1], \\ (\mu-2)^2/4, & \mu \in [1,2). \end{cases} \tag{25}$$

With

$$\mu = \frac{2m}{P}, \quad P \in \mathbb{Z}^+, \quad m \in \{0, \dots, P-1\}, \tag{26}$$

the perturbation (10) has P times the period of the Stokes wave. The spectral stability criterion (25) becomes

$$b \leq \begin{cases} m^2/P^2, & m \in \mathbb{Z} \cap (0, P/2], \\ (m/P-1)^2, & m \in \mathbb{Z} \cap [P/2, P). \end{cases} \tag{27}$$

When $P = 1$, $\mu = 0$ for which the spectral stability criterion is always satisfied. When $P > 1$, the bounds on b are tightest when $m = 1$ and when $m = P-1$, respectively. We call the eigenvalues with $\mu(m=1) = \mu_1$ and $\mu(m = P-1) = \mu_{P-1}$ the critical eigenvalues. In either case we must have

$$b \leq 1/P^2 \tag{28}$$

for spectral stability of Stokes waves with respect to P-subharmonic perturbations (see Figure 1). This result agrees with [16, Theorem 9.1] but is found in a more direct manner.

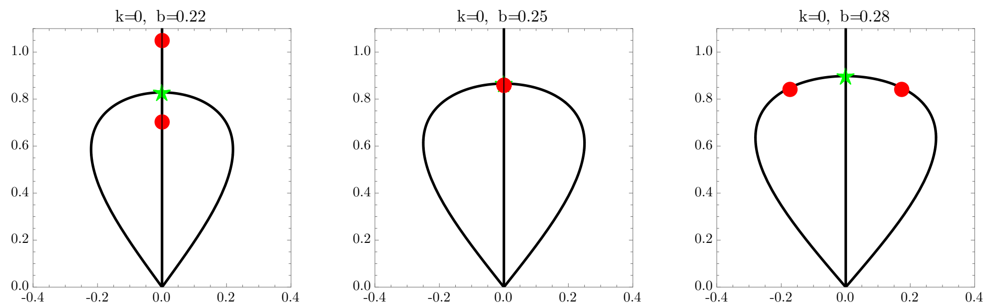

FIG. 2. *The upper half complex λ plane, depicting part of the spectrum for Stokes waves using* (23) *with* $b = 0.22,\ b = 0.25,\ b = 0.28$ *from left to right. Red dots represent eigenvalues with* $P = 2$ *and* $n = 0$ *(using* (26)*). The green star at the intersection of the curve and the imaginary axis represent* λ_c (29) *where the eigenvalues collide.*

Next we examine the process by which solutions transition from a spectrally stable state to a spectrally unstable state with respect to a fixed μ as b increases (see Figure 2). For a fixed $P = P_c$, consider a value of b such that (28) is satisfied with $b < 1/P_c^2$, i.e., the solution is spectrally stable with respect to P_c-subharmonic perturbations. We know from the above that the instability with respect to P_c-subharmonic perturbations first arises when $b_c = 1/P_c^2$ from the critical eigenvalues with $\mu_1 = 2/P_c$ and with $\mu_{P_c-1} = 2(1 - 1/P_c)$. Defining

$$\lambda_c(b) := i\frac{2}{P_c}\sqrt{1-b} = 2i\sqrt{b_c(1-b)}, \tag{29}$$

we find

(30)
$$\operatorname{Im}\left(\lambda_+^{(0,\mu_1)}(b)\right) < \operatorname{Im}(\lambda_c(b)) < \operatorname{Im}\left(\lambda_-^{(0,\mu_1)}(b)\right), \quad \operatorname{Im}\left(\lambda_+^{(-1,\mu_{P_c-1})}(b)\right) > \operatorname{Im}\left(\lambda_c^*(b)\right) > \operatorname{Im}\left(\lambda_-^{(-1,\mu_{P_c-1})}(b)\right):$$

the critical eigenvalues for $n = 0$ and for $n = -1$ are ordered on the imaginary axis and straddle $\lambda_c(b)$ or $\lambda_c^*(b)$. Increasing b leads to $b = b_c = 1/P_c^2$, where

$$\lambda_+^{(0,\mu_1)} = \lambda_-^{(0,\mu_1)} = \lambda_c = -\lambda_+^{(-1,\mu_{P_c-1})} = -\lambda_-^{(-1,\mu_{P_c-1})} \in i\mathbb{R}, \tag{31}$$

and the critical eigenvalues collide at λ_c and $\lambda_c^* = -\lambda_c$ in the upper and lower half planes, respectively. At the collision,

$$\lambda_c(b_c) = 2i\sqrt{b_c(1-b_c)}. \tag{32}$$

This is the intersection of the top of the figure 8 spectrum and the imaginary axis in the complex λ plane [16, equation (92)]. Instability occurs when two critical imaginary eigenvalues collide along the imaginary axis in a Hamiltonian Hopf bifurcation and enter the right and left half planes along the figure 8; see Figure 2. Other such collisions of eigenvalues occur at the top and bottom of the figure 8, leading to unstable modes as b varies, but the classification of spectral stability versus instability is governed by the first unstable modes.

In the rest of section 3, we generalize these Stokes waves results to the elliptic solutions of (1). Doing so is far more technical, but the main idea remains the same: solutions that are spectrally stable with respect to a given subharmonic perturbation become unstable with respect to that subharmonic perturbation when two imaginary eigenvalues collide at the top of the figure 8 spectrum.

3.3. The Lax spectrum and the squared-eigenfunction connection. The stability of the elliptic solutions is more difficult to analyze than that of the Stokes waves since $\mathcal{L}$ (11) does not have constant coefficients. To determine the spectrum $\sigma_{\mathcal{L}}$, we use the integrability of NLS (see Appendix A). In particular, we use that (2) is obtained by requiring that $\chi_{xt} = \chi_{tx}$ hold, where

$$\chi_x = \begin{pmatrix} -i\zeta & \psi \\ -\psi^* & i\zeta \end{pmatrix} \chi, \qquad \chi_t = \begin{pmatrix} A & B \\ C & -A \end{pmatrix} \chi, \tag{33a}$$

$$A = -i\zeta^2 + \frac{i}{2}|\psi|^2 + \frac{i}{2}\omega, \qquad B = \zeta\psi + \frac{i}{2}\psi_x, \qquad C = -\zeta\psi^* + \frac{i}{2}\psi_x^*. \tag{33b}$$

Equations (33) are known as the Lax pair of the focusing NLS equation.

3.3.1. Finding the Lax spectrum and the squared eigenfunction connection. We say that $\zeta \in \sigma_L$ (the Lax spectrum) if ζ gives rise to a bounded (for $x \in \mathbb{R}$) eigenfunction of (33). To determine these eigenfunctions, we restrict the Lax pair (33) to the elliptic solutions (4) by letting $\psi(x,t) = \phi(x)$. Since now (33) are autonomous in t, let $\chi(x,t) = e^{\Omega t}\varphi(x)$. In order for φ to be nontrivial,

$$\Omega^2 = A^2 + BC = -\zeta^4 + \omega\zeta^2 + c\zeta - \frac{1}{16}\left(4\omega b + 3b^2 + (1-k^2)^2\right). \tag{34}$$

For $\chi(x,t)$ to be a simultaneous solution of (33), we require

$$\begin{aligned} \chi(x,t) &= \begin{pmatrix} \chi_1 \\ \chi_2 \end{pmatrix} = e^{\Omega t}\gamma(x) \begin{pmatrix} -B(x;\zeta) \\ A(x;\zeta) - \Omega \end{pmatrix}, \\ \gamma(x) &= \gamma_0 \exp\left(-\int \mathcal{I}\, \mathrm{d}x\right), \end{aligned} \tag{35}$$

whenever $\langle \mathrm{Re}(\mathcal{I})\rangle = 0$, i.e., $\mathrm{Re}(\mathcal{I})$ has zero average over one spatial period $T(k)$, and γ_0 is a constant. The integrand $\mathcal{I}$ is defined by

$$\begin{aligned} \mathcal{I} &= \frac{i\zeta B(x;\zeta) + (A(x;\zeta) - \Omega)\phi(x) + B_x(x;\zeta)}{B(x;\zeta)} \\ &= \frac{A_x(x;\zeta) - \phi(x)^* B(x;\zeta) - i\zeta(A(x;\zeta) - \Omega)}{A(x;\zeta) - \Omega}. \end{aligned} \tag{36}$$

Two seemingly different definitions for $\mathcal{I}$ are given in (36). The two definitions arise from the fact that (33) defines two linearly dependent differential equations for $\gamma(x)$. The two equivalent definitions for $\mathcal{I}$ follow from χ_1 and χ_2, respectively. The average of $\mathcal{I}$ is computed in [16] using the second representation:

$$I(\zeta) = -\int_0^{T(k)} \mathcal{I}\, \mathrm{d}x = -2i\zeta\omega_1 + \frac{4i(-c + 4\zeta^3 - 2\zeta\omega - 4i\zeta\Omega(\zeta))}{\wp'(\alpha)} \left(\zeta_w(\alpha)\omega_1 - \zeta_w(\omega_1)\alpha\right), \tag{37}$$

where ζ_w is the Weierstrass Zeta function [1, Chapter 23], and α is any solution of

$$\wp(\alpha) = 2i(\Omega(\zeta) + i\zeta^2 - i\omega/6). \tag{38}$$

Note that (37) has the opposite sign of [16, equation (69)] in which it is defined inconsistently. Using

$$(\wp'(\alpha))^2 = -4\left(-c + 4\zeta^3 - 2\zeta\omega - 4i\zeta\Omega(\zeta)\right)^2, \tag{39}$$

(37) is given by the simpler form

$$I(\zeta) = -2i\zeta\omega_1 + 2(\zeta_w(\alpha)\omega_1 - \zeta_w(\omega_1)\alpha)\Gamma, \tag{40}$$

where

$$\Gamma = \frac{2i\left(-c + 4\zeta^3 - 2\zeta\omega - 4i\zeta\Omega(\zeta)\right)}{\wp'(\alpha)}. \tag{41}$$

From (39), $|\Gamma| = 1$. The condition for $\zeta \in \sigma_L$ is

$$\zeta \in \sigma_L \Leftrightarrow \mathrm{Re}(I(\zeta)) = 0. \tag{42}$$

The derivative

$$\frac{\mathrm{d}I}{\mathrm{d}\zeta} = \frac{2E(k) - (1 + b - k^2 + 4\zeta^2)K(k)}{2\Omega(\zeta)}, \tag{43}$$

where

$$E(k) := \int_0^{\pi/2} \sqrt{1 - k^2\sin^2(y)}\,\mathrm{d}y, \tag{44}$$

the complete elliptic integral of the second kind [1, Chapter 19], is used for examining σ_L. Tangent vectors to the curves constituting σ_L are given by the vector

$$\left(\mathrm{Im}\left(\frac{\mathrm{d}I}{\mathrm{d}\zeta}\right), \mathrm{Re}\left(\frac{\mathrm{d}I}{\mathrm{d}\zeta}\right)\right)^T \tag{45}$$

in the complex ζ plane.

When $\zeta \in \sigma_L$, the squared-eigenfunction connection [2, 16] gives the spectrum $\lambda = 2\Omega(\zeta)$ and the corresponding eigenfunctions of $\mathcal{L}$ (11),

$$\begin{pmatrix} U \\ V \end{pmatrix} = \begin{pmatrix} e^{-i\theta(x)}\varphi_1^2 - e^{i\theta(x)}\varphi_2^2 \\ -ie^{-i\theta(x)}\varphi_1^2 - ie^{i\theta(x)}\varphi_2^2 \end{pmatrix}, \tag{46}$$

where $(\varphi_1, \varphi_2)^T = e^{-\Omega t}\chi$. The following theorem establishes that the squared-eigenfunction connection can be used to obtain almost every eigenvalue of $\mathcal{L}$.

THEOREM 1. *All but six solutions of* (11) *are obtained through the squared-eigenfunction connection* (46). *Specifically, all solutions of* (11) *bounded on the whole real line are obtained through the squared-eigenfunction connection, except at* $\lambda = 0$.

Proof. The proof is similar to the proof of [6, Theorem 2]. For a complete proof, see Appendix C.4. ∎

Therefore the condition for spectral stability is that $\Omega(\sigma_L) \subset i\mathbb{R}$.

Remark 2. The explicit eigenfunction representation (46) can be used to construct an explicit representation for the Floquet discriminant which is a commonly used tool for computing σ_L [4, 8, 17, 32]. The Floquet discriminant for NLS and other integrable equations is constructed and analyzed in [40].

To examine the stability with respect to subharmonic perturbations, we need λ in terms of μ. Except for the Stokes waves (section 3.2), we cannot express λ in terms of μ explicitly. Instead, we use an explicit expression for $\mu = \mu(\zeta)$ and the connection between ζ and λ to say something about $\lambda(\mu)$. Equation (112) in [16] gives

$$\begin{aligned} e^{iT(k)\mu(\zeta)} &= \exp\left(-2\int_0^{T(k)} \frac{(A(x)-\Omega)\phi(x)+B_x(x)+i\zeta B(x)}{B(x)}\mathrm{d}x\right) e^{i\theta(T(k))} \\ &= e^{2I(\zeta)+i\theta(T(k))}. \end{aligned} \tag{47}$$

It follows that

$$M(\zeta) := T(k)\mu(\zeta) = -2iI(\zeta) + \theta(T(k)) + 2\pi n, \quad n \in \mathbb{Z}. \tag{48}$$

Here, $\theta(T(k))$ is defined to be continuous at $b = k^2$ by

$$\theta(T(k)) := \begin{cases} \int_0^{T(k)} \frac{c}{R^2(x)}\,\mathrm{d}x, & b > k^2, \\ \pi, & b = k^2. \end{cases} \tag{49}$$

For NTP solutions, the Weierstrass integral formula [7, equation 1037.06] gives

$$\begin{aligned} \theta(T(k)) &= \int_0^{2\omega_1} \frac{c}{e_0 - \wp(x; g_2, g_3)}\,\mathrm{d}x = \frac{4c}{\wp'(\alpha_0)}\left(\alpha_0\zeta_w(\omega_1) - \omega_1\zeta_w(\alpha_0)\right) \\ &= -2i\left(\alpha_0\zeta_w(\omega_1) - \omega_1\zeta_w(\alpha_0)\right), \end{aligned} \tag{50}$$

where

$$\wp(\alpha_0) = e_0 = -\frac{2\omega}{3} = b + e_3, \tag{51}$$

and $\wp'(\wp^{-1}(e_0)) = 2ic$ is obtained from [11, equation (3.51)].

3.3.2. A description of the Lax spectrum. Since the Lax spectrum is used to determine the stability spectrum, a complete description of the Lax spectrum is required for our stability analysis. In what follows, we use the notation

(52a)
$$\zeta_1 = \frac{1}{2}\left(\sqrt{1-b} + i\left(\sqrt{b} - \sqrt{b-k^2}\right)\right), \qquad \zeta_2 = \frac{1}{2}\left(-\sqrt{1-b} + i\left(\sqrt{b} + \sqrt{b-k^2}\right)\right),$$
(52b)
$$\zeta_3 = \frac{1}{2}\left(-\sqrt{1-b} - i\left(\sqrt{b} + \sqrt{b-k^2}\right)\right), \quad \zeta_4 = \frac{1}{2}\left(\sqrt{1-b} - i\left(\sqrt{b} - \sqrt{b-k^2}\right)\right),$$

for the roots of Ω^2 in the first, second, third, and fourth quadrants of the complex ζ plane, respectively (for cn and NTP solutions). We refer to the roots collectively as ζ_j. We rely heavily on [16, Lemma 9.2], which states that $M(\zeta)$ (48) must increase in absolute value along σ_L until a turning point is reached, where $\mathrm{d}I/\mathrm{d}\zeta = 0$. The only turning points occur at $\zeta = \pm\zeta_c$, where

$$\zeta_c^2 := \frac{2E(k) - (1 + b - k^2)K(k)}{4K(k)}. \tag{53}$$

Since $\zeta_c^2 \in \mathbb{R}$, ζ_c is real or imaginary depending on the solution parameters (k, b). We refer to ζ_c as the solution to (53) with $\mathrm{Re}(\zeta_c) \geq 0$ and $\mathrm{Im}(\zeta_c) \geq 0$. We primarily use $-\zeta_c$ in the analysis to follow since the branch of spectrum in the left half plane maps to the outer figure 8 (see Figure 6), which corresponds to the dominant instabilities. Further, $\zeta_c = 0$ when $b = B(k)$, where

$$B(k) := \frac{2E(k) - (1 - k^2)K(k)}{K(k)}. \tag{54}$$

For $b > B(k)$, $\zeta_c \in i\mathbb{R} \setminus \{0\}$, and for $b < B(k)$, $\zeta_c \in \mathbb{R} \setminus \{0\}$. The following lemmas concern the shape of the Lax spectrum and are important in our analysis of the stability of solutions.

Lemma 1. *The Lax spectrum σ_L is symmetric about $\mathrm{Im}\,\zeta = 0$. Further, if $\mu(\zeta)$ increases (decreases) in the upper half plane, then $\mu(\zeta)$ decreases (increases) at the same rate in the lower half plane along σ_L.*

Proof. Though the proof for the symmetry of σ_L comes more directly from the spectral problem, we prove it by other means here to set up the proof for the second part of the lemma.

The tangent line to the curve $\mathrm{Re}(I) = 0$ is given by (45), where

$$\mathrm{Re}\left(\frac{\mathrm{d}I}{\mathrm{d}\zeta}\right) = \frac{2E(k)\Omega_r - K(k)\left(8\zeta_i\zeta_r\Omega_i + (1 + b - k^2 + 4(\zeta_r^2 - \zeta_i^2))\Omega_r\right)}{2(\Omega_i^2 + \Omega_r^2)}, \tag{55a}$$

$$\mathrm{Im}\left(\frac{\mathrm{d}I}{\mathrm{d}\zeta}\right) = \frac{-2E(k)\Omega_i + K(k)\left(-8\zeta_i\zeta_r\Omega_r + (1 + b - k^2 + 4(\zeta_r^2 - \zeta_i^2))\Omega_i\right)}{2(\Omega_i^2 + \Omega_r^2)}, \tag{55b}$$

and Ω_r (Ω_i) and ζ_r (ζ_i) are the real (imaginary) parts of Ω and ζ, respectively. Since

(56)

$$\begin{aligned}
\mathrm{Re}\left(\Omega^2\right) &= -\frac{1}{16}\left(1+3b^2-2k^2+k^4-16c\zeta_r + 4b\omega + 16(\zeta_i^4 + \zeta_r^4 - \zeta_r^2\omega + \zeta_i^2(\omega - 6\zeta_r^2))\right),\\
\mathrm{Im}\left(\Omega^2\right) &= \zeta_i\left(-4\zeta_r^3 + 2\omega\zeta_r + c + 4\zeta_i^2\zeta_r\right),
\end{aligned}$$

only $\mathrm{Im}\left(\Omega^2\right)$ changes sign as $\zeta_i \to -\zeta_i$. It follows that $\Omega_i \to -\Omega_i$ and $\Omega_r \to \Omega_r$ as $\zeta_i \to -\zeta_i$. From (45) and (55),

$$\left(\mathrm{Im}\left(\frac{\mathrm{d}I}{\mathrm{d}\zeta}\right), \mathrm{Re}\left(\frac{\mathrm{d}I}{\mathrm{d}\zeta}\right)\right) \to \left(-\,\mathrm{Im}\left(\frac{\mathrm{d}I}{\mathrm{d}\zeta}\right), \mathrm{Re}\left(\frac{\mathrm{d}I}{\mathrm{d}\zeta}\right)\right) \qquad \text{as} \qquad \zeta_i \to -\zeta_i. \tag{57}$$

Therefore, σ_L looks qualitatively the same from ζ_j to $-\zeta_c$ as it does from ζ_j^* to $-\zeta_c$.

We calculate the directional derivative of $\mu(\zeta)$ along σ_L:

(58)

$$\begin{aligned}
\left(\frac{\mathrm{d}\mu(\zeta)}{\mathrm{d}\zeta_r}, \frac{\mathrm{d}\mu(\zeta)}{\mathrm{d}\zeta_i}\right) \cdot \left(\mathrm{Im}\,\frac{\mathrm{d}I}{\mathrm{d}\zeta}, \mathrm{Re}\,\frac{\mathrm{d}I}{\mathrm{d}\zeta}\right) &= 2\left(\frac{\mathrm{d}\,\mathrm{Im}(I)}{\mathrm{d}\zeta_r}, \frac{\mathrm{d}\,\mathrm{Im}(I)}{\mathrm{d}\zeta_i}\right) \cdot \left(\mathrm{Im}\,\frac{\mathrm{d}I}{\mathrm{d}\zeta}, \mathrm{Re}\,\frac{\mathrm{d}I}{\mathrm{d}\zeta}\right)\\
&= 2\left(\left(\mathrm{Im}\,\frac{\mathrm{d}I}{\mathrm{d}\zeta}\right)^2 + \left(\mathrm{Re}\,\frac{\mathrm{d}I}{\mathrm{d}\zeta}\right)^2\right),
\end{aligned}$$

which is symmetric about $\mathrm{Im}\,\zeta = 0$. ∎

LEMMA 2. *When $b \leq B(k)$, given in* (54), *the branch of the Lax spectrum in the left half plane (right half plane) intersects the real axis at $\zeta = -\zeta_c$ ($\zeta = \zeta_c$).*

Proof. Let $\zeta_r \in \mathbb{R}$ and $\epsilon > 0$. Since the vector field (45) is continuous across the real ζ axis, and since σ_L is vertical at the intersection with the real ζ axis by virtue of (57), we must have

$$\operatorname{Im}\left(\left.\frac{\mathrm{d}I}{\mathrm{d}\zeta}\right|_{\zeta=\zeta_r+i\epsilon}\right) = \operatorname{Im}\left(\left.\frac{\mathrm{d}I}{\mathrm{d}\zeta}\right|_{\zeta=\zeta_r-i\epsilon}\right) \qquad \text{as } \epsilon \to 0. \tag{59}$$

We notice that

$$\Omega^2(\zeta_r \pm i\epsilon) = \Omega^2(\zeta_r) \pm i\epsilon\left(c - 4\zeta_r^3 + 2\zeta_r\omega\right) + \mathcal{O}\left(\epsilon^2\right), \tag{60}$$

so that

$$\Omega(\zeta_r \pm i\epsilon) = \Omega(\zeta_r) \pm \frac{i\epsilon}{2\Omega(\zeta_r)}(c - 4\zeta_r^3 + 2\zeta_r\omega) + \mathcal{O}\left(\epsilon^2\right) = i\Omega_i + \Omega_r + \mathcal{O}\left(\epsilon^2\right), \tag{61}$$

where $\Omega_r = \mathcal{O}(\epsilon)$ since $\Omega(\zeta_r) \in i\mathbb{R}$. By (55b), equation (59) is only satisfied as $\epsilon \to 0$ if

$$\zeta_r = \pm\frac{\sqrt{2E(k) - (1 + b - k^2)K(k)}}{2\sqrt{K(k)}} = \pm\zeta_c. \tag{62}$$ □

The next lemma details the topology of the Lax spectrum. To our surprise, there exist few rigorous results describing the Lax spectrum in the literature even though it has been used in various contexts (see, e.g., [4, 17, 32, 33]). Some representative plots of the Lax spectrum are shown in Figure 3.

LEMMA 3. *The Lax spectrum for the elliptic solutions consists only of the real line and two bands, each connecting two of the roots of Ω.*

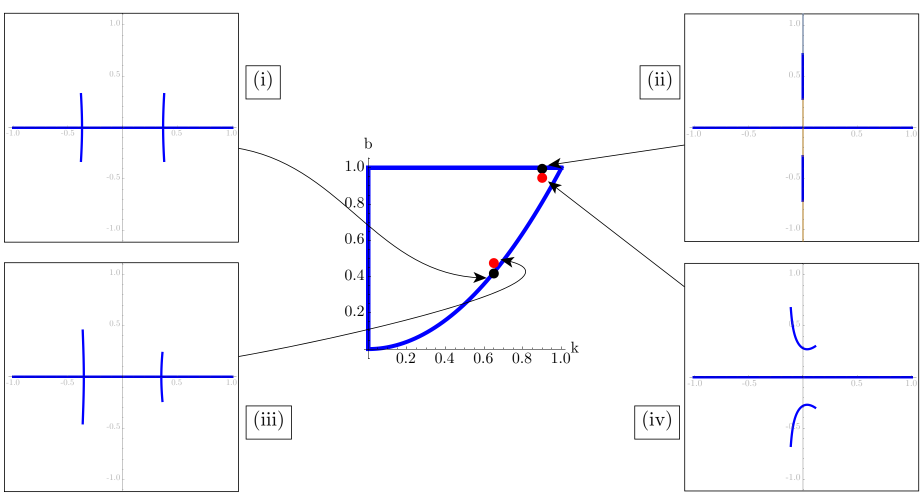

FIG. 3. *Plots of the Lax spectrum.* $\operatorname{Re}\zeta$ *versus* $\operatorname{Im}\zeta$ *for* $\zeta \in \sigma_L$. *Plots* (i) *and* (ii) *are for the cn and dn solutions, respectively. Plots* (iii) *and* (iv) *are for NTP solutions, where the symmetry in all quadrants is broken. Red dots indicate NTP solutions, which are plotted in the lower panels. Parameters are chosen close together to contrast nearby solutions of trivial and nontrivial phase.*

Proof. The fact that the entire real line is part of the Lax spectrum is proven in [16] but we present a different, simpler proof that does not rely on integrating $\mathcal{I}$ (37). If $\zeta \in \mathbb{R}$, the only possibility for a real contribution to the integral of $\mathcal{I}$ over a period $T(k)$ is through

$$\mathcal{E} := \frac{\phi^* B}{A - \Omega}, \tag{63}$$

since $A(x)$ is $T(k)$-periodic. Using the definitions for A, B, and ϕ,

$$\operatorname{Re} \mathcal{E} = \frac{1}{2} \frac{\mathrm{d}}{\mathrm{d}x} \log(R^2 - 2\zeta^2 + \omega + 2i\Omega), \tag{64}$$

which has zero average since R^2 is $T(k)$-periodic. It follows that $\mathbb{R} \subset \sigma_L$. That the roots of $\Omega(\zeta)$ are in the Lax spectrum follows from the fact that $M(\zeta_j) \in \mathbb{R}$ (Lemma 11). Because the coefficients of $\mathcal{L}$ are periodic, there can exist no isolated eigenvalues of $\sigma_{\mathcal{L}}$. It follows that the Lax spectrum can be continued away from the roots of Ω. In what follows, we explain the shape of the spectrum emanating from the roots of Ω and show that these branches and $\mathbb{R}$ constitute the Lax spectrum.

The operator (33) is a second-order differential operator, so it has two linearly independent solutions. The solutions obey

$$\chi_1(x;\zeta) \sim \begin{pmatrix} e^{-i\zeta x} \\ 0 \end{pmatrix}, \qquad \chi_2(x;\zeta) \sim \begin{pmatrix} 0 \\ e^{i\zeta x} \end{pmatrix} \qquad \text{as} \qquad |\zeta| \to \infty. \tag{65}$$

As $|x| \to \infty$, the above two solutions are bounded if and only if $\zeta \in \mathbb{R}$. Therefore, $\mathbb{R}$ is the only unbounded component of σ_L. We examine all possibilities for the finite components of σ_L in the next two paragraphs.

Finite components of the spectrum can terminate only when $\mathrm{d}I/\mathrm{d}\zeta \to \infty$ by the implicit function theorem. This occurs only at the roots of Ω. A component of the spectrum can cross another component only when $\mathrm{d}I/\mathrm{d}\zeta = 0$. This occurs only at ζ_c, which is real if the conditions of Lemma 2 are satisfied and imaginary otherwise. It follows that the spectral bands emanating from the roots of Ω must intersect either the real or the imaginary axis. For the dn solutions, this band lies entirely on the imaginary axis (see section 3.4.1.1). Since there are no other points at which $\mathrm{d}I/\mathrm{d}\zeta = 0$, there can be no other nonclosed curves in the spectrum. However, we must still rule out closed curves along which it is not necessary that $\mathrm{d}I/\mathrm{d}\zeta = 0$ anywhere.

Since I is an analytic function away from the roots of Ω and $\zeta = \infty$, $\operatorname{Re} I$ is a harmonic function of ζ away from the roots of Ω, which we will deal with next. Therefore, if the spectrum contained a closed curve, we would have $\operatorname{Re} I = 0$ on the interior of that closed curve by the maximum principle for harmonic functions. If this were true, then it must also be that the directional derivative of $I(\zeta)$ vanishes on the interior of the region bounded by the closed curve. However, $\mathrm{d}I/\mathrm{d}\zeta = 0$ only at two points which are either on the real or the imaginary axis (53). It follows that there are no closed curves in σ_L disjoint from the roots of Ω. If there were a closed curve which was tangent to the roots of Ω, the above argument would not hold since $\operatorname{Re} I$ is not analytic at the root. However, such a curve would imply that the origin of $\sigma_{\mathcal{L}}$ has multiplicity greater than 4 (the origin has multiplicity 4 since the four roots of Ω map to the origin). This is not possible since $\mathcal{L}$ is a fourth-order differential operator, and such a tangent curve cannot exist. ∎

Remark 3. The above result may also be proven by examining the large-period limit of (4) which is the soliton solution of (1). The spectrum of the soliton is well known [28]. Using the results of [21, 38, 43], the spectrum of the periodic solutions with large period can be understood. Once the spectrum for solutions with large period is understood, the analysis presented in this paper applies and can be extended to solutions with smaller period by continuity.

LEMMA 4. *$0 \leq M(\zeta) < 2\pi$ for $\zeta \in \sigma_L \setminus \mathbb{R}$ with equality only at the end of the bands, when $\Omega(\zeta) = 0$.*

Proof. See Appendix C.3. ∎

Remark 4. We note that Lemma 4 can be rephrased in the language of the Floquet discriminant approach [4, 8, 17, 32] as the nonexistence of *periodic eigenvalues* (those with $M(\zeta) = 0 \mod 2\pi$) on the interior of the complex bands of spectra for the elliptic solutions. Before this result, three things were known about the existence of periodic eigenvalues on the complex bands: (i) The number of periodic eigenvalues on the complex bands was known to have an explicit bound [32]; (ii) for the symmetric solutions (our cn and dn solutions), the number of periodic eigenvalues is zero [8]; and (iii) the nonexistence of periodic eigenvalues on the complex band had been verified numerically [8, 31]. Lemma 4 settles this question: there are no periodic eigenvalues on the complex bands of the Lax spectrum for the elliptic NLS solutions.

3.4. Spectral stability of the elliptic solutions. Results about spectral stability with respect to subharmonic perturbations are found in [16, section 9]. There, sufficient conditions for stability with respect to subharmonic perturbations are found in Theorems 9.1, 9.3, 9.4, 9.5, and 9.6 for spectra with different topology. In this section we present these known sufficient conditions for spectral stability while providing more detailed proofs. For some choices of parameters we show that the sufficient condition is necessary and we comment on progress made toward showing that this condition is necessary for the entire parameter space in Appendix C.

We begin by showing that $\Omega : \mathbb{R} \cap \sigma_L \mapsto \sigma_{\mathcal{L}} \cap i\mathbb{R}$, and therefore the real line of the Lax spectrum always maps to stable modes. Showing that these (and the roots of Ω) are the only parts of the Lax spectrum mapping to stable modes is an important challenge (see Appendix C).

LEMMA 5. *If $\zeta \in \mathbb{R}$, then $\Omega(\zeta) \in i\mathbb{R}$.*

Proof. If $\zeta \in \mathbb{R}$, then the matrix defining the t-evolution in (33) is skew-adjoint, and separation of variables yields imaginary Ω. ∎

Remark 5. The above result is proven in [16]. We present the proof above because it is significantly simpler and is extendable to other stationary solutions of the AKNS hierarchy. Work is currently in progress to extend this and other arguments in this paper to other equations, both in the AKNS hierarchy and not [40].

3.4.1. Trivial-phase solutions, $b = 1$ (dn solutions) or $b = k^2$ (cn solutions). The trivial-phase solutions have $c = 0$ so that

$$\Omega^2(\zeta) = -\zeta^4 + \omega\zeta^2 - \frac{1}{16}\left(4\omega b + 3b^2 + (1-k^2)^2\right), \tag{66}$$

and $\Omega^2(\zeta) = \Omega^2(-\zeta)$. Since $\Omega^2(i\mathbb{R}) \subset \mathbb{R}$, $\lambda(\zeta)$ is real or imaginary for $\zeta \in i\mathbb{R}$. Along with Lemmas 1 and 3, this implies that trivial-phase solutions have symmetric Lax spectrum across both the real and imaginary axes (see Figure 3).

3.4.1.1. *Solutions of dn-type, $b = 1$.* When $b = 1$, $\zeta_j \in i\mathbb{R}$ (52) and

$$\operatorname{Im}(\zeta_2) > \operatorname{Im}(\zeta_1) > 0 > \operatorname{Im}(\zeta_4) > \operatorname{Im}(\zeta_3), \tag{67}$$

with $\zeta_2 = -\zeta_3$ and $\zeta_1 = -\zeta_4$. The following lemmas are needed. The proofs are found in Appendix B.

LEMMA 6. *$M(\zeta_j) = T(k)\mu(\zeta_j) = 0 \mod 2\pi$ for the dn solutions.*

LEMMA 7. *Let $\zeta \in i\mathbb{R}$ with either $|\mathrm{Im}(\zeta)| \geq \mathrm{Im}(\zeta_2)$ or $|\mathrm{Im}(\zeta)| \leq \mathrm{Im}(\zeta_1)$. Then $\Omega(\zeta) \in i\mathbb{R}$.*

The above lemmas allow us to find necessary and sufficient conditions on the spectral stability of dn solutions.

THEOREM 2. *The dn solutions ($b = 1$) are spectrally stable with respect to perturbations of the same period as the underlying solution and no other subharmonic perturbations.*

Proof. Lemmas 3, 7, and the tangent vectors (45) show that the complex bands of the Lax spectrum are confined to the imaginary axis between the roots of Ω. Using Lemmas 4 and 6 and the fact that $M(\zeta)$ must increase in absolute value between the roots of $\Omega(\zeta)$, $M(\zeta) \in [0, 2\pi]$ on the bands of the Lax spectrum. Equality is attained only at the roots ζ_j. By Lemma 7, $\Omega(\zeta) \in \mathbb{R}$ on the interior of the bands, so the eigenvalues are unstable. Since $\zeta \in \mathbb{R}$ only maps to stable modes (Lemma 5), spectral stability only exists for $T(k)\mu = 0$, which is what we wished to show. ∎

3.4.1.2. *Solutions of cn-type, $b = k^2$.* When $b = k^2$, the inequality

$$\Omega^2(i\xi) = -\xi^4 + \frac{1}{2}(2k^2 - 1)\xi^2 - 1/16 < 0 \tag{68}$$

is satisfied for all $\xi \in \mathbb{R}$. We need the following lemmas, whose proofs can be found in Appendix B.

LEMMA 8. *For cn solutions, when $\zeta \in i\mathbb{R}$, $M(\zeta) = \pi \mod 2\pi$.*

LEMMA 9. *$M(\zeta_j) = T(k)\mu(\zeta_j) = 0 \mod 2\pi$ for the cn solutions.*

LEMMA 10. *For $b = k^2$ and $\zeta \in \sigma_L \setminus (\{\zeta_1, \zeta_2, \zeta_3, \zeta_4\} \cup \mathbb{R} \cup i\mathbb{R})$, we have that $\Omega(\zeta) \notin i\mathbb{R}$.*

The above lemmas allow us to find necessary and sufficient conditions on the spectral stability of cn solutions.

THEOREM 3. *If $k > k^* \approx 0.9089$ where k^* is the unique root of $2E(k) - K(k)$ for $k \in [0, 1)$, then solutions of cn-type ($b = k^2$) are spectrally stable with respect to coperiodic and 2-subharmonic perturbations, but no other subharmonic perturbations. If instead $k \leq k^*$, then solutions are spectrally stable with respect to perturbations of period $QT(k)$ for all $Q \in \mathbb{N}$ with $Q \leq P \in \mathbb{N}$ if and only if*

$$M(-\zeta_c) \leq \frac{2\pi}{P}, \tag{69}$$

defined in the 2π-interval in which $M(\zeta_j) = 0$.

Proof. First choose a solution by fixing k. Then choose a P-subharmonic perturbation. If $k > k^*$, then $2E(k) - K(k) < 0$ so that $b > B(k)$ and $\zeta_c \in i\mathbb{R}$ ((54) when $b = k^2$). If $k \leq k^*$, $\zeta_c \in \mathbb{R}$. Consider the band of the spectrum with endpoint ζ_2 at which $M(\zeta_2) = 0$ (Lemma 9). If $\zeta_c \in i\mathbb{R}$, this band intersects the imaginary axis at $\hat{\zeta} \in i\mathbb{R}$; otherwise it intersects the real axis at $-\zeta_c \in \mathbb{R}$.

Let S represent the band connecting ζ_2 to $\hat{\zeta}$ when $\zeta_c \in i\mathbb{R}$. When $\zeta_c \in i\mathbb{R}$, $|\mathrm{Re}(\lambda)| > 0$ on S (Lemma 10) so every $T(k)\mu$ value on S corresponds to an unstable eigenvalue. Since $\mu \neq 0 \mod 2\pi$ on S (Lemma 4), $M(\zeta)$ is increasing from ζ_2 to $\hat{\zeta}$ [16, Lemma 9.2], and $\partial S = \{0, \pi\}$ (Lemmas 8 and 9), $M(\zeta) \in (0, \pi)$ on the interior of S. Therefore every $T(k)\mu \in (0, \pi)$ corresponds to an unstable eigenvalue. By the symmetry of the Lax spectrum in each quadrant, the analysis beginning at any of the roots ζ_j gives the same result, except perhaps with $(0, \pi)$ replaced with $(\pi, 2\pi)$, which yields the same stability results. Since $\mathrm{Re}(\lambda(\zeta)) = 0$ only at $T(k)\mu = 0$, or $T(k)\mu = \pi$, if $2E(k) - K(k) < 0$, the cn solutions are spectrally stable with respect to coperiodic and 2-subharmonic perturbations, but no other subharmonic perturbations.

If $2E(k) - K(k) \geq 0$, the band emanating from ζ_2 intersects the real axis at $-\zeta_c$ (Lemma 2). Then $M(\zeta) \in (0, T(k)\mu(-\zeta_c))$ along the interior of this band and $M(\zeta) = 0$ and $M(\zeta) = T(k)\mu(-\zeta_c)$ at the respective endpoints (Lemma 9). Since $|\mathrm{Re}(\lambda)| > 0$ on the interior of this band (Lemma 10), every $T(k)\mu$ value along this band corresponds to an unstable eigenvalue. By Lemma 4, $M(-\zeta_c) < 2\pi$. Therefore, in order to have spectral stability with respect to P-subharmonic perturbations, it must be that $M(-\zeta_c)$ is at least as small as the smallest nonzero μ value obtained in (26) for our P. The smallest nonzero μ value corresponds to $m = 1$ or $m = P - 1$, so if

$$M(-\zeta_c) \leq \frac{2\pi}{P}, \tag{70}$$

then solutions are spectrally stable with respect to perturbations of period $PT(k)$. Since the Lax spectrum is symmetric about the real and imaginary axes for the cn solutions (see Figure 3(i)), the same bound is found by starting the analysis at each ζ_j. Since the preimage of all eigenvalues with $\mathrm{Re}(\Omega(\zeta)) > 0$ is the interior of the bands (Lemma 10), (70) is also a necessary condition for spectral stability. Since the bound holds for each $Q \leq P$, $Q \in \mathbb{N}$, spectral stability with respect to P-subharmonic perturbations also implies spectral stability with respect to Q-subharmonic perturbations. ∎

Remark 6. The calculations throughout this paper use the period of the modulus of the solution, $T(k) = 2K(k)$. However, the cn solution itself (not its modulus) is periodic with period $4K(k)$. When taking this into account, $I(\zeta)$ gets replaced by $2I(\zeta)$, and

$$T(k)\mu(\zeta) = 4iI(\zeta) + 2\pi n. \tag{71}$$

Using (71) for $M(\zeta)$, Theorem 3 can be updated to cover subharmonic perturbations with respect to the period $4K(k)$ of the cn solutions. We find that when $2E(k) - K(k) < 0$, the solutions are spectrally stable with respect to perturbations of period $4K(k)$. The bound (70) may also be updated using (71) and upon letting $T(k) = 4K(k)$. In particular, we recover the cn solution stability results found in [24, 26].

3.4.2. NTP solutions. For the NTP solutions, $c \neq 0$ and Ω is defined by (34). The statement for the stability of NTP solutions is very similar to that for the stability of cn solutions. We begin with a lemma whose proof can be found in Appendix B.

LEMMA 11. *$M_j := M(\zeta_j) = T(k)\mu(\zeta_j) = 0 \mod 2\pi$ for each root $\{\zeta_j\}_{j=1}^4$ of $\Omega(\zeta)$.*

With this lemma, the following sufficient condition for spectral stability of NTP solutions holds.

THEOREM 4. *Consider a solution with parameters k and $b \leq B(k)$ (54). The solution is spectrally stable with respect to perturbations of period $QT(k)$ for all $Q \in \mathbb{N}$, $Q \leq P \in \mathbb{N}$ if*

$$M(-\zeta_c) \leq \frac{2\pi}{P}, \tag{72}$$

defined in the 2π interval in which $M(\zeta_j) = 0$.

Proof. The proof here, much like the statement of the theorem, is similar to the proof of Theorem 3.

Choose a solution by fixing k and $b \leq B(k)$ so that ζ_c is real. Choose a P-subharmonic perturbation. Consider the band of the spectrum with endpoint ζ_2 (see Figure 3(iii), (iv)), at which $M(\zeta_2) = 0$ (Lemma 11), and which intersects the real line at $-\zeta_c$ (Lemmas 3 and 5). Since $M(\zeta)$ is increasing along the band (Lemma 1), $0 < M(\zeta) < T(k)\mu(-\zeta_c)$ along the interior of the band with $M(\zeta) = 0$ and $M(\zeta) = T(k)\mu(-\zeta_c) < 2\pi$ (Lemma 4) at the respective endpoints.

Since the tangent lines of σ_L are nonvertical at the origin for $b < B(k)$ and $|\mathrm{Re}(\lambda(-\zeta_c \pm i\epsilon))| > 0$ [16], there exist ζ on the bands in a neighborhood of $-\zeta_c$ and a neighborhood of ζ_2 which correspond to eigenvalues λ with $\lambda_r > 0$, i.e., unstable eigenvalues. Since there exist unstable eigenvalues on this band, in order to have spectral stability with respect to P-subharmonic perturbations, it must be that $M(-\zeta_c)$ is at least as small as the smallest nonzero μ obtained in (26) for our P. The smallest nonzero μ value corresponds to $m = 1$ or $m = P - 1$, so if

$$M(-\zeta_c) \leq \frac{2\pi}{P}, \tag{73}$$

then solutions are spectrally stable with respect to perturbations of period $PT(k)$.

By Lemma 1, the same bound is found for the starting point ζ_3. Starting at ζ_1 or ζ_4 gives the bound

$$M(\zeta_c) \leq \frac{2\pi}{P}. \tag{74}$$

However, since

$$M(-\zeta_c) > M(\zeta_c), \tag{75}$$

as shown in [16], the tighter bound is found with $M(-\zeta_c)$. This is the sufficient condition for spectral stability. As for the cn case, if the bound is satisfied for P, then it is also satisfied for all $Q \leq P$. ∎

Remark 7. Determining whether or not the bound (72) is also a necessary condition for spectral stability is a significant challenge. Work in this direction is presented in Appendix C.1.

Remark 8. We note that Lemma 1 implies that near $-\zeta_c \in \mathbb{R}$, two eigenvalues with the same $|T(k)\mu|$ value are found equidistant from $-\zeta_c$ along the band above and below the real axis. Since two eigenvalues with the same $|T(k)\mu|$ mod 2π value represent the same perturbation of period $PT(k)$, the eigenvalues associated with a perturbation of period $PT(k)$ straddle $-\zeta_c$ on either of the arcs and come together or separate as the solution parameters vary; see Figure 4.

THEOREM 5. *If $b > B(k)$ (54), solutions are spectrally stable with respect to coperiodic perturbations. Additionally, they can be spectrally stable with respect to perturbations of twice the period, but they are not stable with respect to any other subharmonic perturbations.*

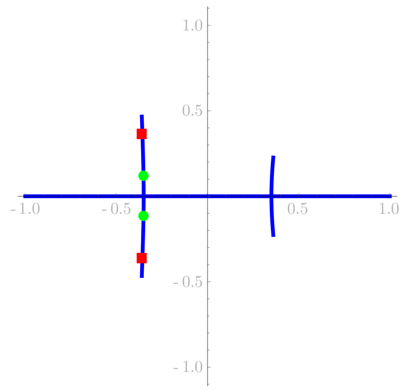

FIG. 4. *The Lax spectrum for* $(k, b) = (0.65, 0.48)$. *Green circles map to eigenvalues of* $\mathcal{L}_\pi$ *(elements of* σ_π *(18)) through* $\Omega(\zeta)$ *(34). In other words,* $P = 2$ *and* $T(k)\mu = \pi$. *Red squares map to eigenvalues of* $\mathcal{L}_{2\pi/3}$*:* $P = 3$ *and* $T(k)\mu = 2\pi/3$. *See Remark* 8.

Proof. See Appendix C.2. ∎

Remark 9. Numerical evidence suggests that when $b > B(k)$, NTP solutions are spectrally stable with respect to coperiodic perturbations and no other subharmonic perturbations. However, there are some parameter values for which the stability spectrum intersects the imaginary axis at a point. We cannot rule out the possibility of this point corresponding to 2-subharmonic perturbations. For the cn solutions, this intersection point corresponds to $M(\zeta) = \pi$, which gives rise to spectral stability with respect to 2-subharmonic perturbations. Because of this, a cn solution and an NTP solution with $b > B(k)$ can be arbitrarily close to each other but have different stability properties. One way to rule out this spurious stability for NTP solutions with $b > B(k)$ is to show that the point $M(\zeta) = \pi$, which we know occurs exactly once on the band of Lax spectrum in the upper half plane, remains in the left half plane (see Lemma 15) for all parameter values.

Having put the subharmonic stability results from [16] on a rigorous footing, we summarize the findings in Figure 5. Equality in condition (72) defines a family of "stability curves," for $P \in \mathbb{N}$, in the parameter space which split up the parameter space into regions bounded by these different curves. The dashed curve shows where $\zeta_c = 0$. Below (above) the dashed curve, ζ_c is real (imaginary). The lightest shading represents spectral stability with respect to coperiodic perturbations: all solutions are spectrally stable with respect to such perturbations [19]. Darker shaded regions represent where solutions additionally are spectrally stable with respect to perturbations of higher multiples of the fundamental period. The P labels inside of the parameter space indicate which solutions are spectrally stable with respect to P-subharmonic perturbations in the given region.

4. The advent of instability. Many results on the spectral stability of the elliptic solutions with respect to subharmonic perturbations were shown in [16]. However, no explanation is given there as to how a solution which is spectrally stable with respect to subharmonic perturbations loses stability as its parameters are varied. We show here that as the amplitude increases, the instabilities of elliptic solutions arise in the same manner as was demonstrated for the Stokes waves (section 3.2). We begin by using the Floquet–Fourier–Hill method [13] to compute the point spectrum for a single subharmonic perturbation (18) (Figure 6). We show that two eigenvalues

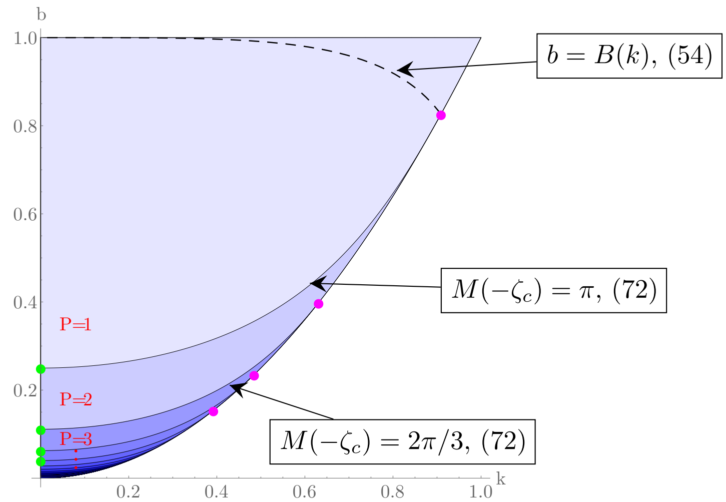

Fig. 5. *The parameter space split up into different regions of subharmonic spectral stability. Each solid curve separating regions of different color corresponds to equality in* (72) *for different values of P. Curves end at $b = 1/P^2$ (green), the stability bound* (28) *for Stokes waves. The magenta dots, along the curve $b = k^2$, show where the stability curves, which are the boundary of different stability regions, intersect the cn solution regime. The dashed line corresponds to* (54)*. Below it, $\zeta_c \in \mathbb{R} \setminus \{0\}$ and above it $\zeta_c \in i\mathbb{R} \setminus \{0\}$.*

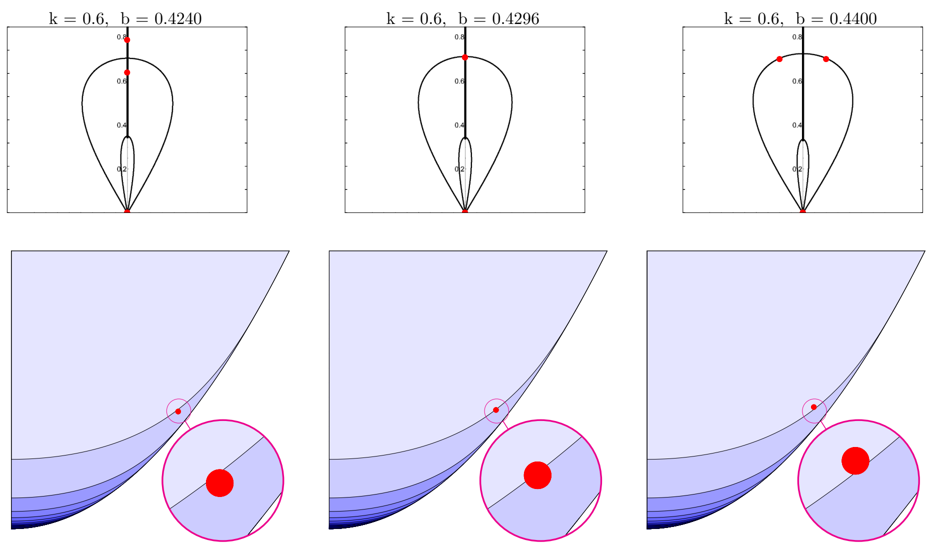

Fig. 6. *For $k = 0.6$ and $P = 2$ (perturbations of twice the period) we vary b to go from spectrally stable to unstable solutions. Top: The top half of the continuous spectrum of $\mathcal{L}$ (black, $\operatorname{Re}\lambda$ versus $\operatorname{Im}\lambda$, plotted using the analytic expression* (42) *and* (34)*) and two eigenvalues with $P = 2$ highlighted with red dots computed using the FFHM. Bottom: Location in parameter space (k versus b).*

collide on the imaginary axis and leave it at the intersection of the figure 8 spectrum and the imaginary axis.

Consider a point (k_Q, b_Q) in the parameter space lying below a stability curve labeled $P = Q$ ($Q = 1, 2, 3, \ldots$), i.e., $M(-\zeta_c(k_Q, b_Q)) < 2\pi/Q$ (see Figure 5). This solution is spectrally stable with respect to perturbations of period $QT(k)$ and the Lax eigenvalues corresponding to Q-periodic perturbations lie on the real axis. Two Lax eigenvalues, $\hat{\zeta}_R$ and $\tilde{\zeta}_R = \hat{\zeta}_R^*$, corresponding to $R > Q$ perturbations lie equidistant from $-\zeta_c(k_Q, b_Q) \in \mathbb{R}$ on the bands connecting to $-\zeta_c(k_Q, b_Q)$ (see Remark 8 and Figure 5). The value $-\zeta_c(k_Q, b_Q)$ lies at the intersection of $\overline{\sigma_L \setminus \mathbb{R}}$ and $\sigma_L \cap \mathbb{R}$ which maps to the intersection of the figure 8 and the imaginary axis in the $\sigma_{\mathcal{L}}$ plane [16]. The stability spectrum eigenvalues, $\hat{\lambda}_R = 2\Omega(\hat{\zeta}_R)$ and $\tilde{\lambda}_R = 2\Omega(\tilde{\zeta}_R)$, corresponding to R-subharmonic perturbations, are on the figure 8 to the left and right of the intersection with the imaginary axis. As the solution parameters are monotonically varied approaching the stability curve which is the boundary of the stability region for R-subharmonic perturbations, where $M(-\zeta_c(k_R, b_R)) = 2\pi/R$, $\tilde{\zeta}_R$ and $\hat{\zeta}_R$ move to $-\zeta_c(k_R, b_R)$, and $\hat{\lambda}_R$ and $\tilde{\lambda}_R$ converge to the top of the figure 8. When this happens, the solution gains spectral stability with respect to perturbations of period $RT(k)$. Spectral stability is gained through a Hamiltonian Hopf bifurcation in which two complex conjugate pairs of eigenvalues come together onto the imaginary axis in the upper and lower half planes.

We are interested in the transition from spectrally stable to unstable solutions. For fixed μ, consider two eigenvalues $\hat{\lambda} = 2\Omega(\hat{\zeta}) \in i\mathbb{R}$ and $\tilde{\lambda} = 2\Omega(\tilde{\zeta}) \in i\mathbb{R}$ spectrally stable). Stability is lost as the solution parameters are varied to cross a stability curve, $\hat{\zeta} \to -\zeta_c$ and $\tilde{\zeta} \to -\zeta_c$, entering a new stability region. The Krein signature [30] gives a necessary condition for two colliding eigenvalues to leave the imaginary axis, leading to instability. For a given eigenvalue λ of the operator $\mathcal{L}_\mu$ associated with a perturbation of period $PT(k)$ and eigenfunction $W = (W_1, W_2)$, the Krein signature is the sign of

$$K_2(\zeta) := \langle W, \mathscr{L}_2 W \rangle = \left\langle W, \hat{H}''(\tilde{r}, \tilde{\ell}) W \right\rangle = \int_{-PT(k)/2}^{PT(k)/2} W^* \hat{H}''(\tilde{r}, \tilde{\ell}) W \, \mathrm{d}x, \tag{76}$$

where $\mathscr{L}_2 = \hat{H}''(\tilde{r}, \tilde{\ell})$ is the Hessian of $\hat{H}(r, \ell)$, defined in Appendix A, evaluated at the elliptic solution.

To relate the eigenfunctions of $J\mathscr{L}_2$ to those of $\mathcal{L}$, we use (118) in Appendix A. Linearizing (118) about the elliptic solution,

$$\begin{pmatrix} r(x,t) \\ \ell(x,t) \end{pmatrix} = \begin{pmatrix} \tilde{r}(x) \\ \tilde{\ell}(x) \end{pmatrix} + \epsilon \begin{pmatrix} w_1(x,t) \\ w_2(x,t) \end{pmatrix} + \mathcal{O}\left(\epsilon^2\right), \tag{77}$$

we obtain

$$\begin{aligned} \frac{\partial}{\partial t} \begin{pmatrix} w_1 \\ w_2 \end{pmatrix} &= \begin{pmatrix} -\tilde{r}\tilde{\ell} & -\frac{1}{2}\partial_x^2 - \frac{1}{2}(\tilde{r}^2 + 3\tilde{\ell}^2) - \omega \\ \frac{1}{2}\partial_x^2 + \frac{1}{2}(3\tilde{r}^2 + \tilde{\ell}^2) + \omega & \tilde{r}\tilde{\ell} \end{pmatrix} \begin{pmatrix} w_1 \\ w_2 \end{pmatrix} \\ &= J\hat{H}''(\tilde{r}, \tilde{\ell}) \begin{pmatrix} w_1 \\ w_2 \end{pmatrix} = J\mathscr{L}_2 \begin{pmatrix} w_1 \\ w_2 \end{pmatrix}. \end{aligned} \tag{78}$$

Separation of variables, $(w_1, w_2)^T = e^{\lambda t}(W_1, W_2)^T$, and the squared-eigenfunction give $\lambda = 2\Omega(\zeta)$ and

$$W = \begin{pmatrix} W_1 \\ W_2 \end{pmatrix} = \begin{pmatrix} \varphi_1^2 + \varphi_2^2 \\ -i\varphi_1^2 + i\varphi_2^2 \end{pmatrix}. \tag{79}$$

From the expressions for the eigenfunctions (46) and (79) it is clear that if an eigenfunction $(U, V)^T$ of $\mathcal{L}$ corresponds to a spectral element λ, then there is a corresponding eigenfunction $(W_1, W_2)^T$ of $J\mathscr{L}_2$ with the same spectral element $\lambda = 2\Omega(\zeta)$.

Since $2\Omega W = J\mathscr{L}_2 W$ and since J is invertible, we find from (79) that

$$W^*\mathscr{L}_2 W = 2\Omega W^* J^{-1} W = 2\Omega(W_1 W_2^* - W_2 W_1^*) = 4i\Omega(|\varphi_1|^4 - |\varphi_2|^4), \tag{80}$$

with $\varphi_1 = -\gamma(x)B(x)$, and $\varphi_2 = \gamma(x)(A(x) - \Omega)$. For a fixed μ and a corresponding spectrally stable solution, $\Omega(\zeta) \in i\mathbb{R}$ for $\zeta \in \mathbb{R}$. When $\zeta \in \mathbb{R}$, the preimage of $\lambda(\zeta) \in i\mathbb{R}$ is only one point (56) so that by Theorem 1, $\lambda(\zeta)$ is a simple eigenvalue. Therefore, we compute the Krein signature only for $\zeta \in \mathbb{R}$. From (35),

$$\gamma(x) = \frac{\gamma_0}{B}\exp(\text{imag})\exp\left(-\int \frac{(A-\Omega)\phi}{B}\,\mathrm{d}x\right), \tag{81}$$

where "imag" represents imaginary terms which are not important for the magnitude of $\gamma(x)$. The magnitude of $\gamma(x)$ depends critically on

$$\begin{aligned} -\frac{(A-\Omega)\phi}{B} = \frac{C\phi}{(A+\Omega)} &= \frac{-i\zeta|\phi|^2 - (\tilde{r}\tilde{r}_x + \tilde{\ell}\tilde{\ell}_x + i\tilde{\ell}\tilde{r}_x - i\tilde{r}\tilde{\ell}_x)/2}{\zeta^2 - |\phi|^2/2 - \omega/2 + i\Omega} \\ &= \text{imag} + \frac{1}{2}\frac{\mathrm{d}}{\mathrm{d}x}\ln|i(A(x)+\Omega)|, \end{aligned} \tag{82}$$

where $\phi = \tilde{r} + i\tilde{\ell}$ is the elliptic solution whose stability is being investigated. Since $A(x) - \Omega \in i\mathbb{R}$, it follows that

$$\gamma(x) = \frac{\gamma_0}{B}\exp(\text{imag})\,|i(A(x)+\Omega)|^{1/2}. \tag{83}$$

Equating $|\gamma_0| = 1$,

$$|\gamma(x)|^2 = \frac{|A+\Omega|}{|B|^2} = \frac{1}{|A-\Omega|}, \tag{84}$$

so that

$$|\varphi_1|^4 = |\gamma|^4|B|^4 = |A+\Omega|^2, \qquad |\varphi_2|^4 = |\gamma|^4|A-\Omega|^4 = |A-\Omega|^2. \tag{85}$$

Further,

$$W^*\mathscr{L}_2 W = 4i\Omega\left(|A+\Omega|^2 - |A-\Omega|^2\right) = -16\Omega^2 iA, \tag{86}$$

implies

$$K_2(\zeta) = -16\Omega^2(\zeta)\int_{-PT(k)/2}^{PT(k)/2}\left(\zeta^2 - \frac{1}{2}|\phi|^2 - \frac{\omega}{2}\right)\,\mathrm{d}x, \tag{87}$$

which is the same K_2 found in [6] with appropriate modifications for the focusing case. This integral can be computed directly using elliptic functions [7, equation (310.01)]:

(88)

$$K_2(\zeta) = -32\Omega^2(\zeta)PT(k)\left(\zeta^2 + \frac{b}{4} + \frac{1}{4}\left(1 - k^2 - 2\frac{E(k)}{K(k)}\right)\right) = -32\Omega(\zeta)^2 PT(k)(\zeta^2 - \zeta_c^2).$$

Note that since $\Omega^2 < 0$ for stable eigenvalues, $K_2(\zeta) < 0$ for $\zeta \in (-\zeta_c, \zeta_c)$ changing sign at $\zeta = \pm\zeta_c$. Therefore the two eigenvalues which collide at $-\zeta_c$ have opposite Krein signatures, a necessary condition for instability.

For the trivial-phase solution, $\Omega(\zeta) = \Omega(-\zeta)$, so the Krein signature calculation here might not be sufficient, since the colliding eigenvalues, $\hat{\lambda}$ and $\tilde{\lambda}$, might not be simple. Our remaining stability results do not rely on this fact. Computing the Krein signature for Stokes waves (section 3.2) is simpler than the calculation here, but it is omitted for brevity.

5. Orbital stability. The results on spectral stability may be strengthened to orbital stability by constructing a Lyapunov functional in conjunction with the results of [22, 34]. In Theorem 4, we have established spectral stability for solutions below the curve (72) (see Figure 5). In this section we show that those solutions are also orbitally stable. To this end, we use the higher-order conserved quantities of NLS (see Appendix A).

DEFINITION. *A stationary solution $\tilde{\Psi}$ of (1) is orbitally stable with respect to the norm $||\cdot||$ if for any given $\epsilon > 0$ there exists a $\delta > 0$ such that*

$$||\Psi(x,0) - \tilde{\Psi}(x,0)|| < \delta \tag{89}$$

implies that for all $t > 0$,

$$\inf_{g \in G} ||\Psi(x,t) - T(g)\tilde{\Psi}(x,t)|| < \epsilon, \tag{90}$$

where $T(g)$ is the action of an element g of the group of symmetries G.

To prove nonlinear stability, we construct a Lyapunov function, i.e., a constant of the motion $\mathcal{K}(r,\ell)$ for which the solution $(\tilde{r},\tilde{\ell})$ is an unconstrained minimizer:

$$\mathcal{K}'(\tilde{r},\tilde{\ell}) = 0, \quad \frac{\mathrm{d}}{\mathrm{d}t}\mathcal{K}(\tilde{r},\tilde{\ell}) = 0, \quad \left\langle v, \mathcal{K}''(\tilde{r},\tilde{\ell})v \right\rangle > 0, \quad \forall v \in \mathbb{V}, v \neq 0. \tag{91}$$

In section 4 it is shown that the energy $\hat{H}$ satisfies the first two conditions in (91) but not the third since K_2 is not of definite sign. When evaluated at stationary solutions, each equation defined in (116) satisfies the first and second conditions. Following the work of [6, 15, 34, 35] we choose one member of (116) to satisfy the third condition by choosing the constants $c_{n,j}$ in a particular manner. A different approach to finding a Lyapunov function is used in [20] for defocusing NLS.

Linearizing the nth NLS equation about the elliptic solution results in

$$w_{t_n} = J\mathscr{L}_n w, \qquad \mathscr{L}_n = \hat{H}_n''(\tilde{r},\tilde{\ell}).$$

The squared-eigenfunction connection and separation of variables give

$$2\Omega_n W(x) = J\mathscr{L}_n W(x), \tag{92}$$

where Ω_n is defined by

$$w(x,t_n) = e^{\Omega_n t_n}\begin{pmatrix} W_1(x) \\ W_2(x) \end{pmatrix} = e^{\Omega_n t_n} W(x) \tag{93}$$

and where $W(x)$ is any eigenfunction of $\mathcal{L}_2$. The relation

$$\Omega_n^2(\zeta) = p_n^2(\zeta)\Omega^2(\zeta), \qquad n \geq 2, \tag{94}$$

where p_n is a polynomial of degree $n-2$, is found in [6] and applies in the focusing case as well. When $n=2$, $p_2=1$ so that $\Omega_2=\Omega$ and (92) implies

$$2J^{-1}W = \frac{1}{\Omega}\mathscr{L}_2 W = \frac{1}{\Omega}\mathscr{L}W, \tag{95}$$

for any eigenfunction W of $\mathcal{L}_2$. The definition of K_2, (76), and (94) imply

(96)

$$K_n(\zeta) := \langle W, \mathscr{L}_n W\rangle = \left\langle W, \hat{H}_n''(\tilde{r},\tilde{\ell})W\right\rangle = \frac{\Omega_n}{\Omega}\int_{-PT(k)/2}^{PT(k)/2} W^*\mathscr{L}_2 W \ \mathrm{d}x = p_n(\zeta)K_2(\zeta).$$

$K_2(\zeta)$ takes the sign $+,-,+$ for $\zeta\in(-\infty,-\zeta_c)$, $\zeta\in(-\zeta_c,\zeta_c)$, and $\zeta\in(\zeta_c,\infty)$, respectively. Since $p_4(\zeta)$ is quadratic, we use $K_4(\zeta)=p_4(\zeta)K_2(\zeta)$, where $p_4(\zeta)$ is defined by (94). Adjusting the constants of p_4 so that it has the same sign as K_2 with zeros at $\zeta=\pm\zeta_c$ makes K_4 nonnegative. In order to calculate $\Omega_4(\zeta)$, we need

$$\hat{T}_4 = T_4 + c_{4,3}T_3 + c_{4,2}T_2 + c_{4,1}T_1 + c_{4,0}T_0, \tag{97}$$

since Ω_4 is defined by $\hat{T}_4\chi=\Omega_4\chi$ by separation of variables in (113e). The $c_{4,k}$ are not entirely arbitrary. They are determined by requiring that the stationary elliptic solutions are stationary with respect to t_4, or

$$\frac{\partial}{\partial t_4}\begin{pmatrix} r\\ \ell\end{pmatrix} = J\hat{H}_4' = J\left(H_4' + c_{4,3}H_3' + c_{4,2}H_2' + c_{4,1}H_1' + c_{4,0}H_0'\right) = 0. \tag{98}$$

Since J is invertible,

$$\hat{H}_4' = H_4' + c_{4,3}H_3' + c_{4,2}H_2' + c_{4,1}H_1' + c_{4,0}H_0' = 0, \tag{99}$$

when evaluated at the stationary solution. Equating

$$0 = \Psi_{\tau_4} + c_{4,3}\Psi_{\tau_3} + c_{4,2}\Psi_{\tau_2} + c_{4,1}\Psi_{\tau_1} + c_{4,0}\Psi_{\tau_0}, \tag{100}$$

and using (113) with Ψ defined in (4), we find

$$c_{4,0} = \omega c_{4,2} - c c_{4,3} + \frac{1}{8}\left(1+15b^2+4k^2+k^4+10b+10bk^2\right), \tag{101a}$$

$$c_{4,1} = \frac{1}{2}c - \frac{1}{2}\omega c_{4,3}, \tag{101b}$$

with $c_{4,2}$ and $c_{4,3}$ arbitrary. Then

$$\Omega_4^2 = \frac{1}{16}\left(2\omega+4\zeta^2+4c_{4,2}+4\zeta c_{4,3}\right)^2\Omega_2^2, \tag{102}$$

so that

$$p_4(\zeta) = \zeta^2 + \zeta c_{4,3} + \frac{1}{2}\omega + c_{4,2}. \tag{103}$$

The constants $c_{4,2}$ and $c_{4,3}$ are chosen so that $K_4(\zeta)=p_4(\zeta)K_2(\zeta)\geq 0$. Setting

$$c_{4,3} = 0, \tag{104a}$$

$$c_{4,2} = -\frac{\omega}{2} + \frac{b}{4} + \frac{1}{4}\left(1-k^2-2\frac{E(k)}{K(k)}\right), \tag{104b}$$

we have

$$K_4(\zeta) = -32\Omega^2(\zeta)PT(k)\left(\zeta^2 - \zeta_c^2\right)^2 \geq 0 \tag{105}$$

for $\zeta \in \mathbb{R}$ and equality only at $\zeta = \pm\zeta_c$ and the roots of Ω. The result (105) has only been proven for eigenfunctions of $\mathcal{L}_2$. However, since the eigenfunctions of $\mathcal{L}_2$ are complete in $L^2_{\text{per}}([-T(k)/2, T(k)/2])$ [25] the results apply to all functions in $L^2_{\text{per}}([-T(k)/2, T(k)/2])$. This result implies that H_4, with the constants chosen above, acts as a Lyapunov functional for the spectrally stable elliptic solutions with respect to the t_4 dynamics. However, since all flows of the NLS hierarchy commute, H_4 is a conserved quantity with respect to the t dynamics as well. Therefore whenever solutions are spectrally stable with respect to a given subharmonic perturbation, they are also formally stable [34].

To go from formal to orbital stability, the conditions of [22] must be satisfied. The kernel of the functional $\hat{H}_4''(\tilde{r}, \tilde{\ell})$ must consist only of the infinitesimal generators of the symmetries of the solution $(\tilde{r}, \tilde{\ell})$. The infinitesimal generators of the Lie point symmetries correspond to the values of ζ for which $\Omega(\zeta) = 0$, so the kernel of $\hat{H}_4''(\tilde{r}, \tilde{\ell})$ contains the infinitesimal generators of the Lie point symmetries. In order for the kernel to consist only of this set, we need strict inequality in (72). This comes from the following lemma.

Lemma 12. *Let b, k, and P be such that* (72) *holds with a strict inequality. Then the set*

$$S := \{\zeta \in \sigma_L : M(\zeta) = m2\pi/P, \quad m = 0, \ldots, P-1\} \tag{106}$$

does not contain $\pm\zeta_c$.

Proof. Since $M(-\zeta_c) < 2\pi/P$, the only possibility for $-\zeta_c$ to be in S is that $M(-\zeta_c) = 0 \mod 2\pi$. But since $-\zeta_c$ represents the intersection of the branch of spectra and the real line, Lemma 4 applies and $M(-\zeta_c) \neq 0 \mod 2\pi$. Since $M(\zeta_c) < M(-\zeta_c)$, it is also the case that ζ_c is not in S ∎

The above lemma implies that if $M(-\zeta_c) < 2\pi/P$, the kernel of $\hat{H}_4''(\tilde{r}, \tilde{\ell})$ consists only of the roots of $\Omega(\zeta)$. It follows that, for a fixed perturbation with period $PT(k)$, all solutions which are spectrally stable with respect to that perturbation and whose parameters do not lie *on* stability curves (the boundary of subharmonic stability regions, at which $M(-\zeta_c) = 2\pi/P$) are also orbitally stable.

Conclusion. We have proven the orbital stability with respect to subharmonic perturbations for the elliptic solutions of the focusing nonlinear Schrödinger equation. The necessary condition for stability (72) is shown to also be a sufficient condition with the help of a numerical check. We see three main remaining tasks to be completed for this problem: (i) remove the numerical check for sufficiency of Theorem 4; (ii) determine whether or not solutions lying on stability curves, $M(-\zeta_c) = 2\pi/P$, are orbitally stable; and (iii) prove that the solutions satisfying $b > B(k)$ in Theorem 5 are not stable with respect to 2-subharmonic perturbations.

The main difficulty in establishing the results presented in this paper is that the Lax pair does not define a self-adjoint spectral problem. Work toward establishing similar nonlinear stability results for the sine-Gordon equation [14], for which the Lax spectral problem is both not self-adjoint and is a quadratic eigenvalue problem, is currently underway. This is generalized in [40] by computing the Floquet discriminant for all equations in the AKNS hierarchy and other integrable equations.

Appendix A. Integrability background. The results presented in this section are found in more detail in classic sources such as [2, 3]. NLS (1) is a Hamiltonian system with canonical variables Ψ and $i\Psi^*$, i.e., it can be written as an evolution equation

$$\frac{\partial}{\partial t}\begin{pmatrix}\Psi\\ i\Psi^*\end{pmatrix} = JH'(\Psi, i\Psi^*) = J\begin{pmatrix}\delta H/\delta\Psi\\ \delta H/\delta(i\Psi^*)\end{pmatrix} \tag{107}$$

for a functional H and where

$$J = \begin{pmatrix}0 & 1\\ -1 & 0\end{pmatrix}. \tag{108}$$

We define the variational gradient [3] of a function $F(u, v)$ by

$$F'(u,v) = \left(\frac{\delta F}{\delta u}\ ,\ \frac{\delta F}{\delta v}\right)^T = \left(\sum_{j=0}^{N}(-1)^j\partial_x^j\frac{\partial F}{\partial u_{jx}}\ ,\ \sum_{j=0}^{N}(-1)^j\partial_x^j\frac{\partial F}{\partial v_{jx}}\right)^T, \tag{109}$$

where $u_{jx} = \partial_x^j u$, and N is the highest-order x-derivative of u or v in F. The quantity $H(\Psi, i\Psi^*)$ is conserved under (1) and is the Hamiltonian of (1). The Hamiltonian is one of an infinite number of conserved quantities of NLS. We label these quantities $\{H_j\}_{j=0}^{\infty}$. We need the first five conserved quantities:

$$H_0 = 2\int |\Psi|^2\ \mathrm{d}x, \tag{110a}$$

$$H_1 = i\int \Psi_x\Psi^*\ \mathrm{d}x, \tag{110b}$$

$$H_2 = \frac{1}{2}\int\left(|\Psi_x|^2 - |\Psi|^4\right)\ \mathrm{d}x, \tag{110c}$$

$$H_3 = \frac{i}{4}\int\left(\Psi_x^*\Psi_{xx} - 3|\Psi|^2\Psi^*\Psi_x\right)\ \mathrm{d}x, \tag{110d}$$

$$H_4 = \frac{1}{8}\int\left(|\Psi_{xx}|^2 - \Psi^2\Psi_x^{*2} - 6|\Psi|^2|\Psi_x|^2 + |\Psi|^2\Psi^*\Psi_{xx} + 2|\Psi|^6\right)\ \mathrm{d}x. \tag{110e}$$

The above equations can be written in terms of Ψ and $i\Psi^*$ by using $|\Psi_{jx}|^2 = \Psi_{jx}\Psi_{jx}^*$. The above integrals are evaluated over one period $T(k)$, for periodic or quasi-periodic solutions. Each H_n defines an evolution equation with respect to a time variable τ_n by

$$\frac{\partial}{\partial\tau_n}\begin{pmatrix}\Psi\\ i\Psi^*\end{pmatrix} = JH_n'(\Psi, i\Psi^*) = J\begin{pmatrix}\delta H_n/\delta\Psi\\ \delta H_n/\delta(i\Psi^*)\end{pmatrix}. \tag{111}$$

When $n = 2$ and $\tau_2 = t$, $H_2 = H$ is the NLS Hamiltonian: (111) is equivalent to (1). Letting $\Psi = (r + i\ell)/\sqrt{2}$ and $i\Psi^* = i(r - i\ell)/\sqrt{2}$, where r and ℓ are the real and imaginary parts of Ψ, respectively, (111) becomes

$$\frac{\partial}{\partial\tau_n}\begin{pmatrix}r\\ \ell\end{pmatrix} = JH_n'(r,\ell) = J\begin{pmatrix}\delta H_n/\delta r\\ \delta H_n/\delta\ell\end{pmatrix}. \tag{112}$$

We use (111) and (112) interchangeably and refer to $H_n(r,\ell)$ and $H_n(\Psi, i\Psi^*)$ as H_n when the context is clear. The collection of equations (111) is the NLS hierarchy [3, section 1.2]. The first five members of the hierarchy are

(113a) $\Psi_{\tau_0} = -2i\Psi,$

(113b) $\Psi_{\tau_1} = \Psi_x,$

(113c) $\Psi_{\tau_2} = i\left|\Psi\right|^2\Psi + \frac{i}{2}\Psi_{xx},$

(113d) $\Psi_{\tau_3} = -\frac{3}{2}\left|\Psi\right|^2\Psi_x - \frac{1}{4}\Psi_{xxx},$

(113e) $\Psi_{\tau_4} = -\frac{3}{4}i|\Psi|^4\Psi - \frac{3}{4}i\Psi^*\Psi_x^2 - \frac{i}{2}\Psi|\Psi_x|^2 - i|\Psi|^2\Psi_{xx} - \frac{i}{4}\Psi^2\Psi^*_{xx} - \frac{i}{8}\Psi_{xxxx}.$

Each equation obtained in this manner is integrable and shares the conserved quantities $\{H_j\}_{j=0}^{\infty}$.

Through the AKNS method, the nth member of the NLS hierarchy is obtained by enforcing the compatibility of a pair of ordinary differential equations, the nth Lax pair. The first equation of the pair is $\chi_{\tau_1} = T_1\chi$ and the second is $\chi_{\tau_n} = T_n\chi$, for the nth member of the hierarchy. Here, T_1 and T_n are 2×2 matrices, the first five of which are defined in (114). The nth member of the NLS hierarchy is recovered by requiring $\partial_{\tau_n}\chi_{\tau_1} = \partial_{\tau_1}\chi_{\tau_n}$. For example, (1) is recovered from the compatibility condition of χ_{τ_1} and χ_{τ_2} with $t = \tau_2$. We call the collection of the Lax equations for the hierarchy the linear NLS hierarchy. The first five members of the linear NLS hierarchy are

(114a)
$$\chi_{\tau_0} = T_0\chi = \begin{pmatrix} -i & 0 \\ 0 & i \end{pmatrix}\chi,$$

(114b)
$$\chi_{\tau_1} = T_1\chi = \begin{pmatrix} -i\zeta & \Psi \\ -\Psi^* & i\zeta \end{pmatrix}\chi,$$

(114c)
$$\chi_{\tau_2} = T_2\chi = \begin{pmatrix} -i\zeta^2 + i\left|\Psi\right|^2/2 & \zeta\Psi + i\Psi_x/2 \\ -\zeta\Psi^* + i\Psi_x^*/2 & i\zeta^2 - i\left|\Psi\right|^2/2 \end{pmatrix}\chi,$$

(114d)
$$\chi_{\tau_3} = T_3\chi$$
$$= \begin{pmatrix} -i\zeta^3 + i\zeta\left|\Psi\right|^2/2 + i\,\mathrm{Im}\left(\Psi\Psi_x^*\right)/2 & \zeta^2\Psi + i\zeta\Psi_x/2 - \left|\Psi\right|^2\Psi/2 - \Psi_{xx}/4 \\ -\zeta^2\Psi^* + i\zeta\Psi_x^*/2 + \left|\Psi\right|^2\Psi^*/2 + \Psi^*_{xx}/4 & i\zeta^3 - i\zeta\left|\Psi\right|^2/2 - i\,\mathrm{Im}\left(\Psi\Psi_x^*\right)/2 \end{pmatrix}\chi,$$

(114e)
$$\chi_{\tau_4} = T_4\chi = \begin{pmatrix} N_1 & N_2 \\ N_3 & -N_1 \end{pmatrix}\chi,$$

where

(115a)
$$N_1 = -i\zeta^4 + i\zeta^2\left|\Psi\right|^2/2 + i\zeta\,\mathrm{Im}(\Psi\Psi_x^*)/2 - 3i\left|\Psi\right|^4/8 + i\left|\Psi_x\right|^2/8 - i\,\mathrm{Re}(\Psi^*\Psi_{xx})/4,$$

(115b)
$$N_2 = \zeta^3\Psi + i\zeta^2\Psi_x/2 - \zeta\left(\left|\Psi\right|^2\Psi/2 + \Psi_{xx}/4\right) - 3i\left|\Psi\right|\Psi_x/4 - i\Psi_{xxx}/8,$$

(115c)
$$N_3 = -\zeta^3\Psi^* + i\zeta^2\Psi_x^*/2 + \zeta\left(\left|\Psi\right|^2\Psi^*/2 + \Psi^*_{xx}/4\right) - 3i\left|\Psi\right|\Psi_x^*/4 - i\Psi^*_{xxx}/8,$$

and ζ is referred to as the Lax parameter.

Each of the H_n are mutually in involution under the canonical Poisson bracket (108) [3]. As a result, the flows of all members of the NLS hierarchy commute and any linear combination of the conserved quantities gives rise to a dynamical equation whose flow commutes with all equations of the hierarchy. We define a family of evolution equations in t_n by

$$\frac{\partial}{\partial_{t_n}}\begin{pmatrix} r \\ \ell \end{pmatrix} = J\hat{H}_n'(r,\ell) = J\left(H_n' + \sum_{j=0}^{n-1} c_{n,j} H_j'\right), \quad n \geq 0, \tag{116}$$

where the $c_{n,j}$ are constants. We loosely call (116) the "nth NLS equation." Similarly we define the nth linear NLS equation to be

$$\chi_{t_n} = \hat{T}_n \chi = \left(T_n + \sum_{j=0}^{n-1} c_{n,j} T_j\right)\chi. \tag{117}$$

The nth NLS equation is obtained by enforcing the compatibility of χ_{τ_1} with χ_{t_n}.

The second NLS equation (2) is obtained from (113a) and (113c) and has Hamiltonian $\hat{H} = \hat{H}_2 = H_2 - \omega H_0/2$. With $\psi(x,t) = (r(x,t) + i\ell(x,t))/\sqrt{2}$, (2) is

$$\partial_t \begin{pmatrix} r \\ \ell \end{pmatrix} = \begin{pmatrix} -\omega\ell - \ell(r^2+\ell^2)/2 - \ell_{xx}/2 \\ \omega r + r(\ell^2 + r^2)/2 + r_{xx}/2 \end{pmatrix} = J\hat{H}'(r,\ell). \tag{118}$$

The associated linear NLS equation is $\hat{T}_2 = T_2 - \omega T_0/2$. Defining $\tau_1 = x$ and $t_2 = t$, (118) (or equivalently (2)) is obtained via the compatibility condition of the two matrix equations

$$\chi_x = \chi_{\tau_1} = T_1 \chi, \tag{119a}$$

$$\chi_t = \chi_{\tau_2} - \frac{\omega}{2}\chi_{\tau_0} = \left(T_2 - \frac{\omega}{2}T_0\right)\chi. \tag{119b}$$

Appendix B. Proofs of some lemmas. In this appendix we present proofs for lemmas used in section 3.4.

Proof of Lemma 6. Formulae for Weierstrass elliptic functions used here and in what follows are in [1, Chapter 23], [7, 42]. We use the notation $\eta_k = \zeta_w(\omega_k)$, $k = 1, 2, 3$.

For the dn solutions, $b = 1$ and the four roots of $\Omega(\zeta)$ are

$$\zeta_1 = \frac{i}{2}\left(1 - \sqrt{1-k^2}\right), \quad \zeta_2 = \frac{i}{2}\left(1 + \sqrt{1-k^2}\right), \quad \zeta_3 = -\zeta_2, \quad \zeta_4 = -\zeta_1. \tag{120}$$

Since $c = \theta = 0$,

$$M(\zeta_j) = -2iI(\zeta_j) \mod 2\pi. \tag{121}$$

The quantities $\alpha(\zeta_j)$, $\wp'(\alpha(\zeta_j))$, and $\zeta_w(\alpha(\zeta_j))$ are needed for the computation of $I(\zeta_j)$. Using (9a) and (38),

(122a)

$$\alpha(\zeta_2) = \alpha(\zeta_3) = \wp^{-1}\left(e_1 + \sqrt{(e_1-e_3)(e_1-e_2)}\right) = \sigma_1 \frac{\omega_1}{2} + 2n\omega_1 + 2m\omega_3,$$

(122b)

$$\alpha(\zeta_1) = \alpha(\zeta_4) = \wp^{-1}\left(e_3 + \frac{(e_3-e_1)(e_3-e_2)}{\wp(\omega_1/2) - e_3}\right) = \sigma_1\left(\frac{\omega_1}{2} - \omega_3\right) + 2n\omega_1 + 2m\omega_3,$$

where $n, m \in \mathbb{Z}$ and σ_1 is either ± 1. From [7, equation 1033.04] and the addition formula for $\wp'(z)$,

$$\wp'(\omega_1/2) = -2\left((e_1-e_3)\sqrt{e_1-e_2} + (e_1-e_2)\sqrt{e_1-e_3}\right) = -2\left(1-k^2+\sqrt{1-k^2}\right), \tag{123a}$$

$$\wp'(\omega_1/2-\omega_3) = 2\left((e_1-e_3)\sqrt{e_1-e_2} - (e_1-e_2)\sqrt{e_1-e_3}\right) = -2\left(1-k^2-\sqrt{1-k^2}\right). \tag{123b}$$

Using the addition formula for $\zeta_w(z)$,

$$\zeta_w(\omega_1/2) = \zeta_w(-\omega_1/2+\omega_1) = -\zeta_w(\omega_1/2) + \eta_1 - \frac{1}{2}\frac{\wp'(\omega_1/2)}{\wp(\omega_1/2)-e_1}, \tag{124}$$

so that

$$\zeta_w(\omega_1/2) = \frac{1}{2}\left(\eta_1 - \frac{1}{2}\frac{\wp'(\omega_1/2)}{\wp(\omega_1/2)-e_1}\right) = \frac{1}{2}\left(\eta_1+1+\sqrt{1-k^2}\right), \tag{125a}$$

$$\zeta_w(\omega_1/2-\omega_3) = \zeta_w(\omega_1/2) - \eta_3 + \frac{1}{2}\frac{\wp'(\omega_1/2)}{\wp(\omega_1/2)-e_3} = \frac{1}{2}\left(\eta_1+1-\sqrt{1-k^2}\right). \tag{125b}$$

Using the parity and periodicity of $\wp'(z)$, and the quasi-periodicity of $\zeta_w(z)$, we arrive at

$$\wp'(\alpha(\zeta_2)) = \sigma_1\wp'(\omega_1/2), \tag{126a}$$

$$\wp'(\alpha(\zeta_1)) = \sigma_1\wp'(\omega_1/2-\omega_3), \tag{126b}$$

$$\zeta_w(\alpha(\zeta_2)) = \sigma_1\zeta_w(\omega_1/2) + 2n\eta_1 + 2m\eta_3, \tag{126c}$$

$$\zeta_w(\alpha(\zeta_1)) = \sigma_1\zeta_w(\omega_1/2-\omega_3) + 2n\eta_1 + 2m\eta_3. \tag{126d}$$

Substituting the above quantities into (37) and using $\omega_3\eta_1 - \omega_1\eta_3 = i\pi/2$ results in $I(\zeta_j) = 0 \mod 2\pi$ for $j = 1, 2, 3, 4$. □

Proof of Lemma 7. Let $\zeta = i\xi$ with $\xi \in \mathbb{R}$. Then

$$\Omega^2(\zeta) = -\xi^4 - \frac{1}{2}(k^2-2)\xi^2 - \frac{k^4}{16} \in \mathbb{R}, \tag{127}$$

so $\Omega(\zeta)$ is either real or imaginary. Then $\Omega(\zeta) \in i\mathbb{R}$ if and only if

$$\xi^2 \geq \frac{1}{4}(2-k^2) + \frac{1}{2}\sqrt{1-k^2} \quad \text{or} \quad \xi^2 \leq \frac{1}{4}(2-k^2) - \frac{1}{2}\sqrt{1-k^2}, \tag{128}$$

which is equivalent to

$$|\xi| \leq \mathrm{Im}(\zeta_1) \quad \text{or} \quad |\xi| \geq \mathrm{Im}(\zeta_2). \tag{129}$$

□

Proof of Lemma 8. First, this holds for $\zeta = 0$, since

$$\alpha(0) = \wp^{-1}(e_3) = \omega_3 + 2n\omega_1 + 2m\omega_2, \tag{130}$$

where $m, n \in \mathbb{Z}$, so that

$$I(0) = 2\Gamma(\omega_1(\eta_3 + 2n\eta_1 + 2m\eta_3) - \eta_1(\omega_3 + 2n\eta_1 + 2m\eta_3) = -\Gamma p\pi i, \tag{131}$$

for $p \in \mathbb{Z}$ [1, Chapter 23]. Then

$$M(\zeta) = -2i(-\Gamma p\pi i) + \pi = \pi \mod 2\pi. \tag{132}$$

Since the curves for $\mathrm{Re}(I)$ = constant, given by (45), and for $\mathrm{Im}(I)$ = constant are orthogonal, the vector field for $\mathrm{Im}(I)$ = constant is vertical on the imaginary axis as $\Omega(\zeta) \in i\mathbb{R}$ there (see (45)). Since $M(\zeta) = \pi \mod 2\pi$ at $\zeta = 0$ and is constant on the imaginary axis, it follows that $M(\zeta) = \pi \mod 2\pi$ on the imaginary axis. □

Proof of Lemma 9. For the cn solutions, $b = k^2$ and the four roots of $\Omega(\zeta)$ are

(133)
$$\zeta_1 = \frac{1}{2}\left(\sqrt{1-k^2} + ik\right), \quad \zeta_2 = \frac{1}{2}\left(-\sqrt{1-k^2} + ik\right), \quad \zeta_3 = -\zeta_1, \quad \zeta_4 = -\zeta_2.$$

Here, $c = 0$ and $\theta(T(k)) = \pi$ give

$$M(\zeta_j) = -2iI(\zeta_j) + \pi \mod 2\pi. \tag{134}$$

The quantities $\alpha(\zeta_j)$, $\wp'(\alpha(\zeta_j))$, and $\zeta_w(\alpha(\zeta_j))$ are needed. Using (9a) and (38),

$$\alpha(\zeta_1) = \alpha(\zeta_3) = \wp^{-1}\left(e_2 - i\sqrt{(e_1-e_2)(e_2-e_3)}\right) = \sigma_1 \frac{\omega_2}{2} + 2n\omega_1 + 2m\omega_3, \tag{135a}$$

$$\begin{aligned}\alpha(\zeta_2) = \alpha(\zeta_3) &= \wp^{-1}\left(e_3 + \frac{(e_3-e_1)(e_3-e_2)}{e_2 - e_3 - i\sqrt{(e_1-e_2)(e_2-e_3)}}\right)\\ &= \sigma_1\left(\frac{\omega_2}{2} - \omega_3\right) + 2n\omega_1 + 2m\omega_3.\end{aligned} \tag{135b}$$

From [7, equation 1033.04] and the addition formula for $\wp'(z)$,

(136a)
$$\begin{aligned}\wp'(\omega_2/2) = -\wp'(\omega_1/2 + \omega_3/2) &= -2\left((e_1-e_2)\sqrt{e_2-e_3} + i(e_2-e_3)\sqrt{e_1-e_2}\right)\\ &= -2k(1-k^2 + ik\sqrt{1-k^2}),\end{aligned}$$

(136b)
$$\wp'(\omega_2/2 - \omega_3) = -2k(1-k^2 - ik\sqrt{1-k^2}).$$

$\zeta_w(\omega_2/2)$ is found in a similar manner to $\zeta_w(\omega_1/2)$ (Lemma 6) to be

$$\zeta_w(\omega_2/2) = \frac{1}{2}\left(\zeta_w(\omega_2) - k + i\sqrt{1-k^2}\right), \tag{137}$$

from which

$$\zeta_w(\omega_2/2 - \omega_3) = \frac{1}{2}\left(\zeta_w(\omega_2) - k - i\sqrt{1-k^2}\right) - \eta_3. \tag{138}$$

Using the parity and periodicity of $\wp'(z)$, and the quasi-periodicity of $\zeta_w(z)$ we arrive at

$$\wp'(\alpha(\zeta_1)) = \sigma_1 \wp'(\omega_2/2), \tag{139a}$$
$$\wp'(\alpha(\zeta_2)) = \sigma_1 \wp'(\omega_2/2 - \omega_3), \tag{139b}$$
$$\zeta_w(\alpha(\zeta_1)) = \sigma_1 \zeta_w(\omega_2/2) + 2n\eta_1 + 2m\eta_3, \tag{139c}$$
$$\zeta_w(\alpha(\zeta_2)) = \sigma_1 \zeta_w(\omega_2/2 - \omega_3) + 2n\eta_1 + 2m\eta_3, \tag{139d}$$

where σ_1 is either ± 1. Substituting the above quantities into (37) results in

$$I(\zeta_1) = I(\zeta_3) = \sigma_1 \frac{i\pi}{2} + 2\pi m, \tag{140a}$$

$$I(\zeta_2) = I(\zeta_4) = 3\sigma_1 \frac{i\pi}{2} + 2\pi m. \tag{140b}$$

Therefore

$$M(\zeta_1) = M(\zeta_3) = \sigma_1 \pi + 4\pi m + \pi = 0 \mod 2\pi, \tag{141a}$$

$$M(\zeta_2) = M(\zeta_4) = 3\sigma_1 \pi + 4\pi m + \pi = 0 \mod 2\pi. \tag{141b}$$

□

Proof of Lemma 10. Without loss of generality, let $\zeta = \zeta_r + i\zeta_i$ with $\zeta_r < 0$. The computation is the same for $\zeta_r > 0$ by symmetry of the Lax spectrum. Consider the curve in the left half plane defined by $\mathrm{Im}(\Omega^2) = 0, \mathrm{Re}(\Omega^2 < 0)$ (56). For $\zeta_i \neq 0$, this curve is defined by

$$\zeta_i^2 = Q(\zeta_r) = \zeta_r^2 - \frac{1}{4}(1 - 2k^2) \qquad \text{for} \qquad \zeta_r \in [-\sqrt{1-k^2}/2, 0). \tag{142}$$

The above parameterization is valid only when $k \geq 1/\sqrt{2}$. For $k < 1/\sqrt{2}$, ζ_r is restricted to a smaller range so that $\zeta_i \in \mathbb{R}$.

Let $G(\zeta_r) = I(\zeta_r + i\zeta_i(\zeta_r))$, where $\zeta_i(\zeta_r)$ is defined with either sign of the square root in (142). If we can show that $\mathrm{Re}(G(\zeta_r)) > 0$ for $\zeta_r \in (-\sqrt{1-k^2}/2, 0)$, then we have shown that $\mathrm{Re}(I(\zeta)) \neq 0$ when $\Omega(\zeta) \in i\mathbb{R} \setminus \{0\}$. We compute

$$4\Omega_i \sqrt{Q(\zeta_r)} \frac{\mathrm{d}\,\mathrm{Re}(G)}{\mathrm{d}\zeta_r} = \zeta_r P_2(\zeta_r), \tag{143}$$

where

$$P_2(\zeta_r) := -16K(k)\zeta_r^2 + 4(E(k) - k^2 K(k)), \tag{144}$$

and

$$\Omega_i := \frac{1}{2}\sqrt{(4\zeta_r^2 + k^2 - 1)(k^2 + 4\zeta_r^2)}, \tag{145}$$

the imaginary part of Ω. Here we take $\Omega_i \sqrt{Q(\zeta_r)} > 0$ without loss of generality ($\Omega_i \sqrt{Q(\zeta_r)} < 0$ corresponds to a different sign for ζ_i or Ω_i or both and is a nontrivial but straightforward extension of what follows). $P_2(\zeta_r)$ and $\mathrm{d}\,\mathrm{Re}(G)/\mathrm{d}\zeta_r$ have opposite signs since $\zeta_r < 0$. Since $\mathrm{Re}(G(-\sqrt{1-k^2}/2)) = 0$ and $P_2(-\sqrt{1-k^2}/2) < 0$, it suffices to show that $\mathrm{d}\,\mathrm{Re}(G)/\mathrm{d}\zeta_r > 0$. Indeed, if this is true, then $\mathrm{Re}(G) > 0$ when $\Omega(\zeta) \in i\mathbb{R} \setminus \{0\}$. There are three cases to consider.

1. Case 1: $P_2(\zeta_r)$ has no negative roots or one root at $\zeta_r = 0$.
   If $P_2(\zeta_r)$ is always negative, then we are done since $\mathrm{Re}(G)$ is increasing on $(-\sqrt{1-k^2}/2, 0)$. This is the case if $E(k) - k^2 K(k) \leq 0$, which is true for $k \geq \kappa$, where $\kappa \approx 0.799879$.
2. Case 2: $P_2(\zeta_r)$ has one negative root and $Q(\zeta_r)$ has no negative roots or a double negative root.
   Let $\hat{\zeta}$ be such that $P_2(\hat{\zeta}) = 0$. Then $\mathrm{Re}(G)$ is increasing on $(-\sqrt{1-k^2}/2, \hat{\zeta})$ and decreasing on $(\hat{\zeta}, 0)$. This can occur only for $1/\sqrt{2} < k < \kappa$. Since

$$\frac{\mathrm{d}\,\mathrm{Re}(I)}{\mathrm{d}\zeta_i} = -\,\mathrm{Im}\left(\frac{\mathrm{d}I}{\mathrm{d}\zeta}\right), \tag{146}$$

$\mathrm{d}\,\mathrm{Re}(I)/\mathrm{d}\zeta_i > 0$ for $\zeta = i\zeta_i$. Since $\mathrm{Re}(G(\zeta_r))$ must be minimized in the limit $\zeta_r \to 0^-$, it follows from continuity and the fact that $\mathrm{Re}(G) > 0$ on the imaginary axis that $\mathrm{Re}(G) > 0$ for $\zeta_r \in (-\sqrt{1-k^2}/2, 0)$.

3. Case 3: $P_2(\zeta_r)$ and $Q(\zeta_r)$ both have one negative root.
   Let $\hat{\zeta}$ be as above and let $\hat{\xi}$ be the negative root of Q. Then $\mathrm{Re}(G)$ is increasing on $(-\sqrt{1-k^2}/2, \hat{\zeta})$ and decreasing on $(\hat{\zeta}, \hat{\xi})$ at which $\mathrm{Re}(G(\hat{\xi})) = 0$. Since the parameterization is not valid on $(\hat{\xi}, 0)$, $\mathrm{Re}(G) > 0$ for $\zeta_r \in (-\sqrt{1-k^2}/2, \hat{\xi})$, which are all allowed ζ values for which $\zeta \notin \mathbb{R} \cup i\mathbb{R}$.

It follows that $\mathrm{Re}(G) > 0$ when $\Omega(\zeta) \in i\mathbb{R} \setminus \{0\}$. ∎

Proof of Lemma 11. We establish that $M_j = 0 \mod 2\pi$ on the boundary of the parameter space by establishing this fact for the Stokes waves ($k = 0$) and using Lemmas 6 and 9.

Setting $\lambda = 0$ in (23) shows that $\mu = -2n$. Since $T(k) = \pi$ for Stokes waves, $T(k)\mu = 0 \mod 2\pi$ whenever $\Omega = 0$. Next, we compute directly that $\partial_b M_j = 0$ for the NTP solutions. In what follows we use that

$$\zeta_j = \frac{1}{2}\left(\sigma_1\sqrt{1-b} + i\sigma_2\left(\sqrt{b} - \sigma_1\sqrt{b-k^2}\right)\right), \tag{147}$$

so that $\zeta_1,\ \zeta_2,\ \zeta_3$, and ζ_4 correspond to $(\sigma_1, \sigma_2) = (1,1),\ (-1,1),\ (-1,-1),\ (1,-1)$, respectively. We define

$$e_{p,j} = \wp(\alpha_j) - e_0 = -2\zeta_j^2 + \omega, \tag{148}$$

where e_0 is defined in (51), and use

$$\frac{\partial \zeta_j}{\partial b} = \frac{e_{p,j}}{4c}, \tag{149a}$$

$$\frac{\partial \alpha_0}{\partial b} = \frac{1}{\wp'(\alpha_0)} = -\frac{i}{2c}, \tag{149b}$$

$$\frac{\partial \alpha_j}{\partial b} = -\frac{c + 2\zeta_j e_{p,j}}{2c\wp'(\alpha_j)} = \frac{4\zeta_j^3 - 2\zeta_j\omega - c}{2c\wp'(\alpha_j)}. \tag{149c}$$

From the definition of Γ and (39),

$$\frac{(4\zeta_j^3 - 2\zeta_j\omega - c)\Gamma}{\wp'(\alpha_j)} = \frac{2i(4\zeta_j^3 - 2\zeta_j\omega - c)^2}{\wp'(\alpha_j)^2} = -\frac{i}{2}. \tag{150}$$

Using the above calculations, the expression (40), and (48) with $\theta(T(k))$ defined in (50), we compute

(151)
$$\begin{aligned}\frac{\partial}{\partial b}M_j &= -2i\left(\frac{\partial I(\zeta_j)}{\partial b} + \frac{\partial}{\partial b}(\alpha_0\eta_1 - \omega_1\zeta_w(\alpha_0))\right)\\ &= -2i\left(-\frac{i}{2c}e_{p,j}\omega_1 - \frac{(4\zeta_j^3 - 2\zeta_j\omega - c)\Gamma}{c\wp'(\alpha_j)}(\eta_1 + \omega_1(e_{p,j} + e_0)) - \frac{i}{2c}(\eta_1 + \omega_1 e_0)\right) = 0\end{aligned}$$

by direct computation. Since $M_j = 0 \mod 2\pi$ along the boundaries of the parameter region (Figure 1) and $\partial_b M_j = 0$ on the interior of the parameter space, it follows that M_j is constant ($0 \mod 2\pi$) in the whole parameter space. ∎

Appendix C. Necessity of stability condition (72), proof of Lemma 4, and proof of Theorem 5. In this appendix we present progress made toward showing that (72) is not only a sufficient but also a necessary condition for spectral stability. We introduce a theorem which shows that $|\mathrm{Re}(\lambda)| > 0$ on the complex bands of the spectrum. For part of the parameter space, the proof of this theorem is complete. For a different part of parameter space, the proof relies upon a numerical check over a bounded region of parameter space (see Figure 8(a)). The numerical check consists of finding a root of a degree-six polynomial and evaluating Weierstrass elliptic functions at that root. Numerical checks of this kind are not uncommon (see, e.g., the nondegeneracy condition for focusing NLS in [19]). We use similar arguments as used in Lemma 13 to prove Theorem 5 and Lemma 4.

Lemma 13. *Let $c \neq 0$ and $\zeta \in (\mathbb{C}^- \cap \sigma_L) \setminus (\mathbb{R} \cup i\mathbb{R} \cup \{\zeta_2, \zeta_3\})$, where $\mathbb{C}^-$ is the left half plane. Then $\Omega(\zeta) \notin i\mathbb{R}$.*

Proof. Let $c \neq 0$ and $\zeta = \zeta_r + i\zeta_i$ with $\zeta_r < 0$. Consider the curve in the left half plane defined by $\mathrm{Im}(\Omega^2) = 0$. For $\zeta_i \neq 0$, this curve is defined by

$$\zeta_i^2 = \zeta_r^2 - \frac{\omega}{2} - \frac{c}{4\zeta_r}. \tag{152}$$

The condition $\mathrm{Re}(\Omega^2) \leq 0$ implies $|\zeta_r| \leq \sqrt{1-b}/2$ with equality attained at the roots of Ω^2. Let

$$Q(\zeta_r) := 4\zeta_r^3 - 2\omega\zeta_r - c. \tag{153}$$

We have that $\zeta_i \in \mathbb{R}$ only if $Q(\zeta_r) \leq 0$ and $Q(\zeta_r)$ has two roots with negative real part. If both roots are complex or there is a double root, then the parameterization (152) is valid for all $-\sqrt{1-b}/2 \leq \zeta_r < 0$. This is the case if the discriminant of Q is nonpositive, which is true when

$$b \geq \begin{cases} k^2, & k > 1/\sqrt{2}, \\ F(k), & k \leq 1/\sqrt{2}, \end{cases} \tag{154}$$

with

$$F(k) := \frac{(1+k^2)^3}{9(1-k^2+k^4)}. \tag{155}$$

It is interesting to note that the condition $b < F(k)$ is the same condition as [16, equation (85)], which determines when the imaginary Ω axis is quadruple covered by the map $\Omega(\zeta)$.

Define $G(\zeta_r) = I(\zeta_r + i\zeta_i(\zeta_r))$, where $\zeta_i(\zeta_r)$ is defined with either sign of the square root in (152). The goal is to show that $\mathrm{Re}\, G(\zeta_r) = 0$ only when $\zeta_i = 0$ or $\zeta_r = -\sqrt{1-b}/2$, which corresponds to one of the roots of Ω^2. Along the solutions of (152),

$$\Omega_i \zeta_r \sqrt{Q(\zeta_r)} \frac{\mathrm{d}\,\mathrm{Re}\, G}{\mathrm{d}\zeta_r} = P_6(\zeta_r), \tag{156}$$

where

$$\Omega_i = \pm \frac{1}{4\,|\zeta_r|} \sqrt{(4\zeta_r^2 + b - 1)(b + 4\zeta_r^2)(b - k^2 + 4\zeta_r^2)}, \tag{157}$$

the imaginary part of Ω (and $\Omega = \Omega_i$ because of the parameterization). The polynomial P_6 is given by

$$P_6(x) = -64K(k)x^6 + 16(E(k) + (k^2 - 2b)K(k))x^4 + 8cK(k)x^3 + 2c(E(k) + (b-1)K(k))x - c^2K(k). \tag{158}$$

We let $\Omega_i\sqrt{Q(\zeta_r)} > 0$, without loss of generality ($\Omega_i\sqrt{Q(\zeta_r)} < 0$ corresponds to a different sign for ζ_i or Ω_i or both and is a nontrivial but straightforward extension of what follows). Therefore, $P_6(\zeta_r)$ has the opposite sign of $\mathrm{d}\,\mathrm{Re}(G)/\mathrm{d}\zeta_r$ and $\mathrm{Re}(G(\zeta_r)) \to +\infty$ as $\zeta_r \to 0^-$ since $\Omega_i\zeta_r\sqrt{Q(\zeta_r)} \to 0^-$ and $P_6 \to -c^2K(k) < 0$. Since $\zeta_r = -\sqrt{1-b}/2$ corresponds to a root of Ω and the roots of Ω are in the Lax spectrum, $\mathrm{Re}\,G(-\sqrt{1-b}/2) = 0$. We wish to show that $\mathrm{d}\,\mathrm{Re}(G)/\mathrm{d}\zeta_r \geq 0$, which guarantees that $\mathrm{Re}(G(\zeta_r)) = 0$ only when $\Omega(\zeta_r) = 0$.

Consider the polynomial

$$\tilde{P}_6(x) = P_6(-x) = a_6x^6 + a_4x^4 + a_3x^3 + a_1x + a_0. \tag{159}$$

It is clear that $a_6 < 0, a_3 < 0, a_0 < 0$ and a_4 changes sign depending on b and k. We have

$$a_1 = -2c\left(E(k) + (b-1)K(k)\right) \leq -2c\left(E(k) + (k^2-1)K(k)\right) = -2c\frac{\mathrm{d}K(k)}{\mathrm{d}k} \leq 0. \tag{160}$$

By Descartes' sign rule, an upper bound on the number of negative roots of P_6 is either 2 or 0, depending on the sign of a_4. Since $P_6(\zeta_r) \to -\infty$ as $\zeta_r \to -\infty$ and $P_6(0) < 0$, $P_6(\zeta_r)$ has an even number of negative roots, either 2 or 0.

We consider four cases.

1. Case 1: $P_6(\zeta_r)$ has no negative roots or a double negative root.
   If $P_6(\zeta_r)$ has no negative roots or a double negative root, then $P_6(\zeta_r) \leq 0$ and $\mathrm{Re}(G(\zeta_r)) > 0$ so $\mathrm{Re}(G(\zeta_r))$ is bounded away from 0 (see Figure 7(a)).
2. Case 2: $P_6(\zeta_r)$ has two distinct negative roots, $Q(\zeta_r)$ has no negative roots.
   Let ξ_1 and ξ_2 be the two roots of P_6 with $\xi_1 < \xi_2 < 0$ (see Figure 7(b)). Then $\mathrm{Re}(G)$ is increasing on $(-\sqrt{1-b}/2, \xi_1)$, decreasing on (ξ_1, ξ_2), and increasing again on $(\xi_2, 0)$. If $\mathrm{Re}(G(\xi_2)) > 0$, then $\mathrm{Re}(G)$ is bounded away from 0 and we are done. We do not know how to verify this condition analytically, so we check it numerically. It is found to always hold.
3. Case 3: $P_6(\zeta_r)$ has two distinct negative roots, $Q(\zeta_r)$ has a double negative root.
   Let ξ_1 and ξ_2 be as above and let ζ_1 be the negative double root of Q (see Figure 7(c)). It must be the case that $\zeta_1 > \xi_1$ since $\mathrm{Re}(G)$ is initially increasing and we know that $\mathrm{Re}(G) \to 0$ as $\zeta \to \zeta_1$. However, since ζ_1 is a double root of Q, it is also a root of $\mathrm{Re}(G)$ so it must be that $\zeta_1 = \xi_2$. This means that $\mathrm{Re}(G)$ is tangent to 0 at $\zeta = \zeta_1$. This corresponds to $\zeta \in \mathbb{R}$.
4. Case 4: $P_6(\zeta_r)$ and $Q(\zeta_r)$ have two distinct negative roots
   Let ξ_1 and ξ_2 be as before and let ζ_1 and ζ_2 be the two negative roots of Q with $\zeta_1 < \zeta_2$. As before, it must be that ξ_1 is smaller than each of ξ_2, ζ_1, and ζ_2. The next largest root may be either ξ_2 or ζ_1.
   - An illustration of this case is found in Figure 7(d). If ξ_2 is the next largest root, then there is a $\hat{\zeta} \in (\xi_1, \xi_2)$ such that $\mathrm{Re}(G(\hat{\zeta})) = 0$. For

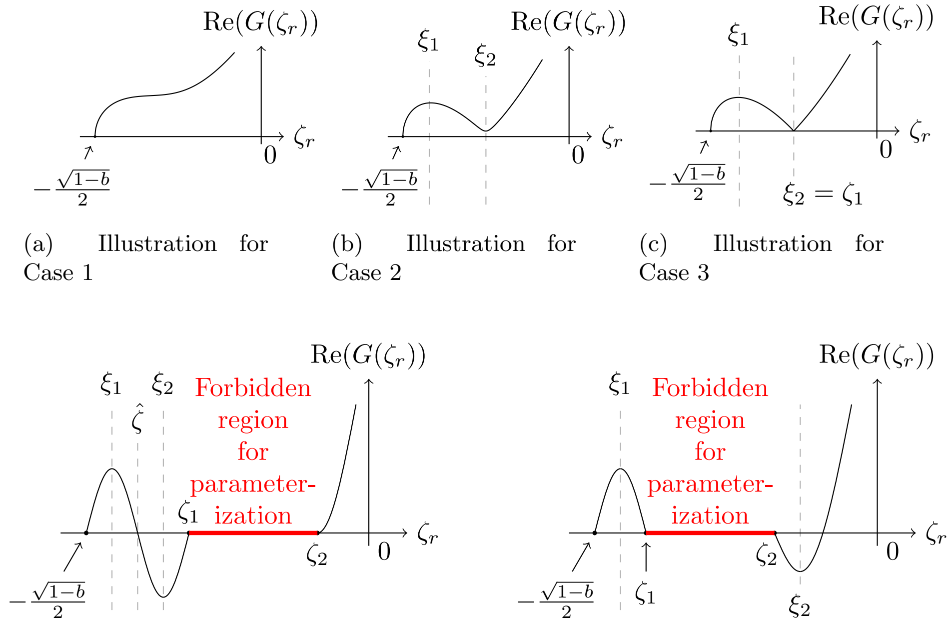

(a) Illustration for Case 1

(b) Illustration for Case 2

(c) Illustration for Case 3

(d) Illustration for Case 4, option 1

(e) Illustration for Case 4, option 2

FIG. 7. *Illustrations of* ζ_r *versus* $\mathrm{Re}(G(\zeta_r))$ *for the four cases in the proof of Lemma* 13.

ζ_r greater than ξ_2, $\mathrm{Re}(G)$ increases to 0 at $\zeta_r = \zeta_1$. For $\zeta \in (\zeta_1, \zeta_2)$, nothing can be said about $\mathrm{Re}(G)$ since the parameterization is not valid. For $\zeta \in (\zeta_1, 0)$, $\mathrm{Re}(G) > 0$ is increasing since $P_6(\zeta) < 0$ in this range. Thus if the ordering is $\xi_1 < \xi_2 < \zeta_1 < \zeta_2$, there is a $\hat{\zeta} \in \sigma_L$ such that $\mathrm{Re}(G(\hat{\zeta})) = 0$ and $\Omega(\hat{\zeta}) \in i\mathbb{R}$.

- An illustration of this case is found in Figure 7(e). If ζ_1 is the next largest root, there are no zeros on $(-\sqrt{1-b}/2, \zeta_1)$. If there were, there would be another zero of P_6 in (ξ_1, ζ_1) (so that $\mathrm{Re}(G)$ can increase back to zero) but there is not, by assumption. For $\zeta_r \in (\zeta_1, \zeta_2)$, the parameterization is not valid. $\mathrm{Re}(G(\zeta_2)) = 0$ and is increasing if $\xi_2 < \zeta_2$ and is decreasing if $\xi_2 > \zeta_2$. If $\mathrm{Re}(G)$ is increasing at ζ_2, we are done. If $\mathrm{Re}(G)$ is decreasing at ζ_2, then since $\mathrm{Re}(G) \to \infty$ as $\zeta_r \to 0$, there must be another zero of $\mathrm{Re}(G)$ in $(\zeta_2, 0)$.

In either of the two subcases of Case 4, there can be at most one $\zeta_r = \hat{\zeta}_r$ with $\mathrm{Re}\, G(\hat{\zeta}_r) = 0$. However, Lemma 14 below shows that there must be an even number of zeros of $\mathrm{Re}(G(\zeta_r))$ for $\zeta_r < 0$. It follows that there must be 0 intersections and Case 4 is eliminated. Since Case 1 and Case 3 also do not pose any problems, we are left with verifying Case 2 only. This check is done numerically for some parameters, which completes the proof of Lemma 13. □

Remark 10. The numerical search required for Lemma 13 need not take place over the whole parameter space. Case 2 can only occur when (154) holds with strict inequality ($b = F(k)$ corresponds to Case 3). Thus our search region covers only those b values satisfying $b > \max(k^2, F(k))$. The search space is shrunk further by looking

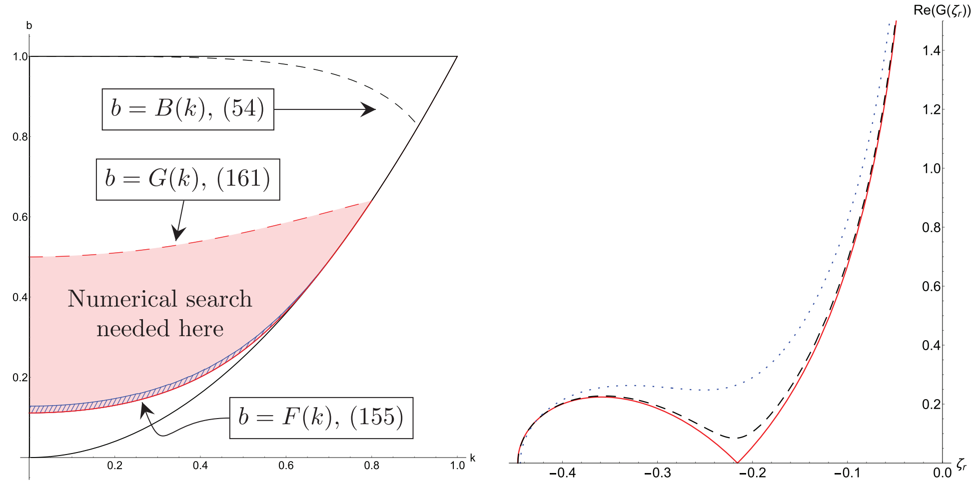

(a) (b)

Fig. 8. (a) *The parameter space with curves indicating when a numerical check to show that the condition* (72) *in Theorem* 4 *is both necessary and sufficient. For more details, see Lemma* 13. *The dashed blue region just above the line* $b = F(k)$ *indicates where* P_6 *has either* 1 *or* 2 *negative roots and hence where the numerical check takes place.* (b) *Plots of* ζ_r *versus* $\mathrm{Re}(G(\zeta_r))$ *near* $b = F(k)$ *for* $k = 0.4$. *The curve* $b = F(k)$ *is shown in solid red,* $b = F(k) + 0.001$ *in dashed black, and* $b = F(k) + 0.01$ *in dotted blue. See Cases* 2 *and* 3 *in the proof of Lemma* 13. *The numerical check in Case* 2 *is to determine whether* $\mathrm{Re}(G(\zeta_r)) = 0$ *anywhere for* $b > F(k)$.

only for those (b, k) pairs satisfying $a_4 > 0$ in (159). $a_4 \le 0$ if and only if $b \ge G(k)$, where

$$G(k) := \frac{E(k) + k^2 K(k)}{2K(k)}. \tag{161}$$

The search region is further shrunk by first checking whether or not P_6 has two negative roots, counted with multiplicity. This check needs to be done numerically since the roots cannot be found analytically. The search region shown in Figure 8(a) indicates where P_6 has two negative roots. From our numerical tests, fewer than 4% of the grid points in the search region give rise to P_6 with negative roots, independent of grid spacing. Therefore, fewer than 4% of the points are checked to satisfy $\mathrm{Re}(G(\xi_2)) > 0$. Representative plots of $\mathrm{Re}(G(\zeta_r))$ near $b = F(k)$ are shown in Figure 8(b). It is verified that, for a grid spacing of 10^{-10}, the condition $\mathrm{Re}(G(\xi_2)) > 0$ is satisfied in the necessary domain. The numerical check can be removed if it can be shown that the minimum of $\mathrm{Re}(G(\zeta_r))$ at ξ_2 is monotonically increasing as b increases from $F(k)$. We are not, however, able to prove that at this time.

C.1. $\zeta_c \in \mathbb{R}$: An extension of Theorem 4. We first look at cases when $b \le B(k)$ (54) so that $\zeta_c \in \mathbb{R}$.

Lemma 14. *Let* $b \le B(k)$ *so that* $\zeta_c \in \mathbb{R}$. *Then for* $\zeta \in (\mathbb{C}^- \cap \sigma_L) \setminus \mathbb{R}$, $\Omega(\zeta)$ *has an even number of intersections with the imaginary* Ω *axis.*

Proof. We note that for $\zeta \in (\mathbb{C}^- \cap \sigma_L) \setminus \mathbb{R}$, $\Omega(\zeta)$ has 0, 1, or 2 intersections with the imaginary axis by Lemma 13. The tangent line to $\sigma_{\mathcal{L}}$ at the origin is given by [16, equation (104)],

$$\frac{\mathrm{d}\Omega_i}{\mathrm{d}\Omega_r} = \pm\frac{(2c-\sqrt{1-b}(k^2-2b))E(k)}{(\sqrt{b-k^2}+\sqrt{b})(1+\sqrt{b(b-k^2)}-b)E(k)+(1-k^2)K(k)}, \tag{162}$$

with $+$ corresponding to ζ_3 and $-$ corresponding to ζ_2. It follows that for ζ near ζ_3 on σ_L, the stability spectrum enters the first quadrant of the λ plane. For $\zeta \in \sigma_L \setminus \mathbb{R}$ near $-\zeta_c \in \mathbb{R}$, $\zeta = -\zeta_c + i\delta_i + \mathcal{O}\left(\delta_i^2\right)$, where $\delta_i \in \mathbb{R}$ is a small perturbation parameter [16, equation (150)]. A short calculation gives

$$\Omega(-\zeta_c + i\delta_i) = \Omega(-\zeta_c) + \frac{i}{2}\frac{\delta_i}{\Omega(-\zeta_c)}(4\zeta_c^3 - 2\omega\zeta_c + c), \tag{163}$$

where $\Omega(-\zeta_c) \in i\mathbb{R}$. Then

(164)

$$\begin{aligned}4\zeta_c^3 - 2\omega\zeta_c + c &= \sqrt{\frac{2E(k)-(b-k^2+1)K(k)}{2K^3(k)}}\left(4E(k)+K(k)(b+k^2-3)\right)\\ &= \sqrt{\frac{2E(k)-(b-k^2+1)K(k)}{2K^3(k)}}\left(k(k')^2\frac{\mathrm{d}K(k)}{\mathrm{d}k}+2E(k)-K(k)\right) \geq 0,\end{aligned}$$

since $b < B(k)$. Since $\sigma_{\mathcal{L}}$ enters the first quadrant from the origin and enters the imaginary axis from the first quadrant, it must have an even number of crossings with the imaginary axis. In particular there must be either 0 or 2 crossings. ∎

Using Theorem 4, Lemmas 13 and 14 imply that the condition (72) is both a necessary and a sufficient condition for spectral stability when $2E(k) - (1 + b - k^2)K(k) \geq 0$ by following the exact same proof as for Theorem 3.

Theorem 6. *The sufficient condition for spectral stability* (72) *given in Theorem* 4 *is also necessary.*

Proof. Using Lemma 13 we see that $\Omega(\zeta) \in i\mathbb{R}$ for $\zeta \in \sigma_L \cap \mathbb{C}^-$ if and only if $\zeta \in \mathbb{R} \cup \{\zeta_1, \zeta_2\}$. This means that the bound (72) is a necessary and sufficient condition for spectral stability. When $\max(k^2, F(k)) < b < G(k)$, Lemma 13 relies upon a numerical check. ∎

Remark 11. If one is not pleased working with the numerical check, then the results in this appendix only change in the following manner. The bound (72) still determines which solutions are spectrally stable with respect to perturbations of period $PT(k)$. It still follows that if $Q < P$ and a solution is stable with respect to perturbations of period $PT(k)$, then this solution is also spectrally stable with respect to perturbations of period $QT(k)$. The results in the appendix are only needed to rule out spectral stability with respect to other perturbations, e.g., perturbations with period $RT(k)$ for $R > P$.

C.2. A proof of Theorem 5, $\zeta_c \in i\mathbb{R}$. In this subsection we present the details needed to establish Theorem 5.

Lemma 15. *Let $c \neq 0$, $\zeta_c \in i\mathbb{R}$, and $\zeta \neq \zeta_1$ be in the open first quadrant. Then $\Omega(\zeta) \in i\mathbb{R}$ for at most one value of $\zeta \in \sigma_L$.*

Proof. The proof is similar to that of Lemma 13 with the following changes. Here $Q(\zeta_r)$ always has one zero for $\zeta_r > 0$. Call this zero $\hat{\zeta}$. Then the parameterization (152) is valid for $\zeta_r \in [\hat{\zeta}, \sqrt{1-b}/2]$. We find that $P_6(\zeta_r)$ has at most two positive zeros by Descartes' sign rule. Since $P_6(\zeta_r)$ has at most two positive zeros and we know that $\mathrm{Re}(G(\hat{\zeta})) = \mathrm{Re}(G(\sqrt{1-b}/2)) = 0$, it follows that there is at most one other ζ_r value at which $\mathrm{Re}(G) = 0$. ◻

Proof of Theorem 5. We note that if $2E(k) - (1 + b - k^2)K(k) < 0$, then $\zeta_c \in i\mathbb{R}$ and it must be that σ_L intersects $i\mathbb{R}\backslash\{0\}$ (Lemma 3; see Figure 3(iv)). Let $\hat{\zeta} \in i\mathbb{R}\backslash\{0\}$ be the intersection point of σ_L and $i\mathbb{R} \setminus \{0\}$. Since $\mathrm{Re}(\hat{\zeta}) = 0$ and $\mathrm{Im}(\hat{\zeta}) \neq 0$, (56) implies that $\Omega(\hat{\zeta}) \notin i\mathbb{R}$. By (57), $M(\zeta)$ is increasing on (ζ_2, ζ_1) except perhaps at ζ_c if $\zeta_c \in \sigma_L$. In any case, since $M(\zeta_2) = M(\zeta_1) = 0 \mod 2\pi$, $M(\zeta)$ traces out all of $T(k)\mu \in (0, 2\pi)$. By Lemma 13, $\mathrm{Re}(\lambda) > 0$ for $\zeta \in (\zeta_2, \hat{\zeta}]$. By Lemma 15, $\mathrm{Re}(\lambda) = 0$ at most at one point in the band connecting ζ_2 to ζ_1. Since we need $\mathrm{Re}(\lambda) = 0$ for $P - 1$ different μ values different from 0 for stability by (26), it follows that there can be stability at most for $P = 2$. Since $P = 2$ corresponds to perturbations of twice the period, we have arrived at the desired result.

Finally, we note that the above proof does not rely on the numerical check in Lemma 13 since the curve $b = B(k)$ (see (54)) always lies above the curve $b = G(k)$ (see (161)) for $k^2 < b < 1$. To see this, we note that $B(k) > G(k)$ if and only if

$$3E(k) - 2(k')^2K - k^2K(k) > 0. \tag{165}$$

But

$$3E(k) - 2(k')^2K(k) - k^2K(k) > \frac{\pi k^2}{4}\frac{2(1-k^2)^{-3/8} - (1-k^2/4)^{-1/2}}{(1-k^2/4)^{1/2}(1-k^2)^{3/8}} > 0 \tag{166}$$

for $0 < k < \tilde{k} \approx 0.941952$, where all estimates are found in [1, section 19.4]. It can be verified that both $B(\tilde{k}) < \tilde{k}^2$ and $G(\tilde{k}) < \tilde{k}^2$, so we have $B(k) > G(k)$ everywhere in the domain $k^2 < b < 1$, hence no numerical check is needed for solutions satisfying $b > B(k)$. ◻

C.3. A proof of Lemma 4.

Proof of Lemma 4. For the cn solutions and the NTP solutions with $b \leq F(k)$ (see (155)) or $b \geq G(k)$ (see (161)), Lemmas 10 and 13 imply that every $\zeta \in (\mathbb{C}^- \cap \sigma_L) \setminus \mathbb{R}$ gives rise to an unstable eigenvalue $\lambda(\zeta)$. By [19], the elliptic solutions are spectrally stable with respect to coperiodic perturbations. Since coperiodic perturbations correspond to $T(k)\mu = 0 \mod 2\pi$, we conclude that in the cases above $M(\zeta) \neq 0$ for ζ on the complex bands of the Lax spectrum in the left half plane. It is left to show that the same result holds for the NTP solutions with $F(k) < b < G(k)$.

By continuity, an eigenvalue with $T(k)\mu = 0 \mod 2\pi$ (hereafter called a *periodic eigenvalue*) can only enter a complex band by passing through the intersection of the complex band with the real axis. Since a periodic eigenvalue has $\mathrm{Re}(\Omega(\zeta)) = 0$ by [19], it must be the case that the curve (152) intersects the complex band at a periodic eigenvalue. Since the intersection of (152) and the complex band must occur immediately upon the periodic eigenvalue entering the band, it must be that the curve (152) and the complex band intersect the real axis at the same location, $\zeta = -\zeta_c$ (see (53)). The curve (152) intersects the real axis when $Q(\zeta_r) = 0$ (see (153)). But $Q(\zeta_r) = 0$ only at the boundary of the region $F(k) < b < G(k)$, when $b = F(k)$. Therefore, in order to establish that no periodic eigenvalues enter the complex band, we must establish that the zero of $Q(\zeta_r)$ mentioned above is not equal to $-\zeta_c$.

When $b = F(k)$, $Q(\zeta_r)$ has a double zero at $\zeta_r = \tilde{\zeta}_1 < 0$:

$$Q(\zeta_r) = 4(\zeta_r - \tilde{\zeta}_1)^2(\zeta_r - \tilde{\zeta}_2). \tag{167}$$

Comparing the above expression to (153), we find that $\tilde{\zeta}_1^2 = \omega/6$. But

$$\zeta_c^2 - \tilde{\zeta}_1^2 = 2\left(E(k) - \frac{1}{3}(2-k^2)K(k)\right) \tag{168}$$

$$\geq E(k) - \frac{2}{3}K(k) > \sqrt{1-k^2}K(k) - \frac{2}{3}K(k) > 0 \tag{169}$$

for $k^2 < 5/9$ (the inequality used for $E(k)$ comes from [1, section 19.9]). Since $b = F(k) < k^2$ only when $k^2 < 1/2 < 5/9$, we find that the intersection of $Q(\zeta_r)$ with the real line is well separated from the intersection of the complex band with the real line for all allowed k. It follows that no periodic points can enter the complex band in the left half plane. We finish the proof by noting that since $2\pi > M(-\zeta_c) > M(\zeta_c)$, periodic points also cannot enter the complex band in the right half plane. ∎

C.4. A proof of Theorem 1.

Proof of Theorem 1. The proof is similar to the proof of [6, Theorem 2]. We provide details omitted there.

For every $\lambda \in \mathbb{C}$, (11) can be written as a four-dimensional first-order system of ordinary differential equations. For each $\lambda \in \mathbb{C}$, one value of Ω is obtained through $\Omega = \lambda/2$. Defining

$$\tilde{Q}_4(\zeta) := -\zeta^4 + \omega\zeta^2 + c\zeta - \frac{1}{16}\left(4\omega b + 3b^2 + (1-k^2)^2\right) \tag{170}$$

and

$$Q_4(\Omega, \zeta) := \Omega^2 - \tilde{Q}_4(\zeta), \tag{171}$$

we let

$$\mathcal{B} := \{\lambda \in \mathbb{C} : \text{ the discriminant of } Q_4 \text{ with respect to } \zeta \text{ vanishes}\}. \tag{172}$$

For $\lambda \in \mathbb{C} \setminus \mathcal{B}$, the zeros of $Q_4(\Omega, \zeta)$ give four values of $\zeta \in \mathbb{C}$. It is not necessary that each of these four values of ζ is in the Lax spectrum since this counting argument is independent of the Lax spectrum. The squared-eigenfunction connection (46) gives a solution to (11) for each of the four $\zeta \in \mathbb{C}$. Therefore, (46) gives four solutions of the fourth-order problem (11) for each $\lambda \in \mathbb{C} \setminus \mathcal{B}$. We first show that the four solutions obtained through (46) are linearly independent for $\lambda \in \mathbb{C} \setminus \mathcal{B}$, then later we will look at $\lambda \in \mathcal{B}$.

Using the fact that

$$B_x = 2(-i\zeta B - \phi A), \tag{173}$$

the eigenfunctions (35) may be written as

$$\begin{aligned} \chi(x,t) &= e^{\Omega t}\begin{pmatrix} -B \\ A - \Omega \end{pmatrix} \gamma_0 \exp\left(-\int \left(\frac{B_x}{2B} + \frac{\phi\Omega}{B}\right)\, \mathrm{d}x\right) \\ &= e^{\Omega t}\begin{pmatrix} -B \\ A - \Omega \end{pmatrix} \frac{\gamma_0}{B^{1/2}} \exp\left(-\int \frac{\phi\Omega}{B}\, \mathrm{d}x\right). \end{aligned} \tag{174}$$

When $\lambda \in \mathbb{C} \setminus (\mathcal{B} \cup \{0\})$, the above gives four eigenfunctions, one for each ζ. The four eigenfunctions have singularities at the zeroes of B. Since the zeros of B depend on ζ, the four eigenfunctions have different singularities in the complex x plane for the four different values of ζ. When $\Omega = 0$, there exist two bounded eigenfunctions [19, Proposition 3.2]. Only one of these is obtained through (35).

We now consider the six values of $\lambda \in \mathcal{B}$. The discriminant can vanish only in one of the following cases:

1. $Q_4 = (\zeta - \hat{\zeta}_1)(\zeta - \hat{\zeta}_2)(\zeta - \hat{\zeta}_3)^2 = 0$,
2. $Q_4 = (\zeta - \hat{\zeta}_1)^2(\zeta - \hat{\zeta}_2)^2 = 0$,
3. $Q_4 = (\zeta - \hat{\zeta}_1)(\zeta - \hat{\zeta}_2)^3 = 0$, or
4. $Q_4 = (\zeta - \hat{\zeta}_1)^4 = 0$. □

The zeros of Q_4 come from level sets of $\tilde{Q}_4(\zeta)$. Case 4 can occur only when the graph of $\tilde{Q}_4(\zeta)$ has one maximum. However, since we know from (52) that all four roots of $\tilde{Q}_4(\zeta)$ cannot be equal, case 4 is not possible. Case 3 can also be ruled out since the four roots (52) of $\tilde{Q}_4(\zeta)$ are real. Case 2 can occur only when two roots of (52) collide, which can occur only for the cn or dn solutions. The stability of these cases has been determined [24] so they are not a concern here. Finally, case 1 is possible. In case 1, only three values of ζ are determined from Ω. In such a case, three linearly independent solutions of (11) are found. The fourth is obtained using reduction of order and introduces algebraic growth so it is not an eigenfunction. Therefore in this case, all eigenfunctions are found using the squared-eigenfunction connection.

Acknowledgments. The authors acknowledge Greg Forest, Stephane Lafortune, and Vishal Vasan for helpful conversations and ideas. In addition, the referees are thanked for many useful suggestions. Any opinions, findings, and conclusions or recommendations expressed in this material are those of the authors and do not necessarily reflect the views of the funding sources.

REFERENCES

[1] F. W. J. Olver, A. B. Olde Daalhuis, D. W. Lozier, B. I. Schneider, R. F. Boisvert, C. W. Clark, B. R. Miller and B. V. Saunders, eds., *NIST Digital Library of Mathematical Functions*, Release 1.0.14, http://dlmf.nist.gov/.

[2] M. Ablowitz, D. Kaup, A. Newell, and H. Segur, *The inverse scattering transform-Fourier analysis for nonlinear problems*, Stud. Appl. Math., 53 (1974), pp. 249–315.

[3] M. Ablowitz and H. Segur, *Solitons and the Inverse Scattering Transform*, SIAM Stud. Appl. Math. 4, SIAM, Philadelphia, 1981.

[4] M. J. Ablowitz, B. M. Herbst, and C. M. Schober, *Computational chaos in the nonlinear Schrödinger equation without homoclinic crossings*, Phys. A, 228 (1996), pp. 212–235, https://doi.org/10.1016/0378-4371(95)00434-3.

[5] N. Bottman and B. Deconinck, *KdV cnoidal waves are spectrally stable*, Discrete Contin. Dyn. Syst., 25 (2009), pp. 1163–1180, https://doi.org/10.3934/dcds.2009.25.1163.

[6] N. Bottman, B. Deconinck, and M. Nivala, *Elliptic solutions of the defocusing NLS equation are stable*, J. Phys. A, 44 (2011), 285201, https://doi.org/10.1088/1751-8113/44/28/285201.

[7] P. Byrd and M. Friedman, *Handbook of Elliptic Integrals for Engineers and Physicists*, Grundlehren Math. Wiss. 67, Springer, New York, 2013.

[8] A. Calini, S. Keith, and S. Lafortune, *Squared eigenfunctions and linear stability properties of closed vortex filaments*, Nonlinearity, 24 (2011), pp. 3555–3583, https://doi.org/10.1088/0951-7715/24/12/011.

[9] T. Cazenave and P.-L. Lions, *Orbital stability of standing waves for some nonlinear Schrödinger equations*, Comm. Math. Phys., 85 (1982), pp. 549–561, http://projecteuclid.org/euclid.cmp/1103921547.

[10] F. Chen, *Introduction to Plasma Physics*, Springer, New York, 2012.

[11] R. Conte and M. Musette, *The Painlevé Handbook*, Springer, New York, 2008.

[12] B. Deconinck and T. Kapitula, *The orbital stability of the cnoidal waves of the Korteweg-de Vries equation*, Phys. Lett. A, 374 (2010), pp. 4018–4022, https://doi.org/10.1016/j.physleta.2010.08.007.

[13] B. Deconinck and J. Kutz, *Computing spectra of linear operators using the Floquet-Fourier-Hill method*, J. Comput. Phys., 219 (2006), pp. 296–321, http://dx.doi.org/10.1016/j.jcp.2006.03.020.
[14] B. Deconinck, P. McGill, and B. L. Segal, *The stability spectrum for elliptic solutions to the sine-Gordon equation*, Phys. D, 360 (2017), pp. 17–35.
[15] B. Deconinck and M. Nivala, *The stability analysis of the periodic traveling wave solutions of the mKdV equation*, Stud. Appl. Math., 126 (2011), pp. 17–48, http://dx.doi.org/10.1111/j.1467-9590.2010.00496.x.
[16] B. Deconinck and B. L. Segal, *The stability spectrum for elliptic solutions to the focusing NLS equation*, Phys. D, 346 (2017), pp. 1–19, https://doi.org/10.1016/j.physd.2017.01.004.
[17] N. Ercolani and D. McLaughlin, *Toward a topological classification of integrable PDEs*, in The Geometry of Hamiltonian Systems (Berkeley, CA, 1989), Math. Sci. Res. Inst. Publ., 22, Springer, New York, 1991, pp. 111–129, https://doi.org/10.1007/978-1-4613-9725-0_9.
[18] T. Gallay and M. Hărăguş, *Stability of small periodic waves for the nonlinear Schrödinger equation*, J. Differential Equations, 234 (2007), pp. 544–581, https://doi.org/10.1016/j.jde.2006.12.007.
[19] T. Gallay and M. Hărăguş, *Orbital stability of periodic waves for the nonlinear Schrödinger equation*, J. Dynam. Differential Equations, 19 (2007), pp. 825–865, https://doi.org/10.1007/s10884-007-9071-4.
[20] T. Gallay and D. Pelinovsky, *Orbital stability in the cubic defocusing NLS equation:* I. *Cnoidal periodic waves*, J. Differential Equations, 258 (2015), pp. 3607–3638, https://doi.org/10.1016/j.jde.2015.01.018.
[21] R. A. Gardner, *Spectral analysis of long wavelength periodic waves and applications*, J. Reine Angew. Math., 491 (1997), pp. 149–181, https://doi.org/10.1515/crll.1997.491.149.
[22] M. Grillakis, J. Shatah, and W. Strauss, *Stability theory of solitary waves in the presence of symmetry.* I, J. Funct. Anal., 74 (1987), pp. 160–197, https://doi.org/10.1016/0022-1236(87)90044-9.
[23] E. P. Gross, *Structure of a quantized vortex in boson systems*, Nuovo Cimento (10), 20 (1961), pp. 454–477.
[24] S. Gustafson, S. Le Coz, and T. Tsai, *Stability of periodic waves of* 1*D cubic nonlinear Schrödinger equations*, Appl. Math. Res. Express. AMRX, 2017, pp. 431–487, https://doi.org/10.1093/amrx/abx004.
[25] M. Hărăguş and T. Kapitula, *On the spectra of periodic waves for infinite-dimensional Hamiltonian systems*, Phys. D, 237 (2008), pp. 2649–2671, https://doi.org/10.1016/j.physd.2008.03.050.
[26] T. Ivey and S. Lafortune, *Spectral stability analysis for periodic traveling wave solutions of NLS and CGL perturbations*, Phys. D, 237 (2008), pp. 1750–1772, https://doi.org/10.1016/j.physd.2008.01.017.
[27] T. Kapitula, *On the stability of N-solitons in integrable systems*, Nonlinearity, 20 (2007), pp. 879–907, https://doi.org/10.1088/0951-7715/20/4/005.
[28] D. Kaup, *Perturbation theory for solitons in optical fibers*, Phys. Rev. A, 42 (1990), p. 5689.
[29] Y. Kivshar and G. Agrawal, *Optical Solitons: From Fibers to Photonic Crystals*, Academic Press, New York, 2003.
[30] R. Kollár and P. D. Miller, *Graphical Krein signature theory and Evans-Krein functions*, SIAM Rev., 56 (2014), pp. 73–123, https://doi.org/10.1137/120891423.
[31] S. Lafortune, *personal communication*, 2018.
[32] J. J. Lee, *The Inverse Spectral Solution, Modulation Theory and Linearized Stability Analysis of n-Phase, Quasi-Periodic Solutions of the Nonlinear Schrodinger Equation*, Ph.D. thesis, Ohio State University, 1986.
[33] Y. Ma and M. Ablowitz, *The periodic cubic Schrödinger equation*, Stud. Appl. Math., 65 (1981), pp. 113–158, https://doi.org/10.1002/sapm1981652113.
[34] J. Maddocks and R. Sachs, *On the stability of KdV multi-solitons*, Comm. Pure Appl. Math., 46 (1993), pp. 867–901, https://doi.org/10.1002/cpa.3160460604.
[35] M. Nivala and B. Deconinck, *Periodic finite-genus solutions of the KdV equation are orbitally stable*, Phys. D, 239 (2010), pp. 1147–1158, https://doi.org/10.1016/j.physd.2010.03.005.
[36] L. Pitaevskii, *Vortex lines in an imperfect Bose gas*, Sov. Phys. JETP, 13 (1961), pp. 451–454.
[37] G. Rowlands, *On the stability of solutions of the non-linear Schrödinger equation*, IMA J. Appl. Math., 13 (1974), pp. 367–377, https://doi.org/10.1093/imamat/13.3.367.
[38] B. Sandstede and A. Scheel, *On the stability of periodic travelling waves with large spatial period*, J. Differential Equations, 172 (2001), pp. 134–188, https://doi.org/10.1006/jdeq.2000.3855.

[39] C. Sulem and P.-L. Sulem, *The Nonlinear Schrödinger Equation: Self-Focusing and Wave Collapse*, Appl. Math. Sci. 139, Springer, New York, 2007.

[40] J. Upsal and B. Deconinck, *Real Lax Spectrum Implies Spectral Stability*, in preparation, 2019.

[41] M. Weinstein, *Lyapunov stability of ground states of nonlinear dispersive evolution equations*, Comm. Pure Appl. Math., 39 (1986), pp. 51–67, https://doi.org/10.1002/cpa.3160390103.

[42] E. Whittaker and G. Watson, *A Course of Modern Analysis*, Cambridge University Press, Cambridge, UK, 1996.

[43] Z. Yang and K. Zumbrun, *Convergence as Period Goes to Infinity of Spectra of Periodic Traveling Waves Toward Essential Spectra of a Homoclinic Limit*, preprint, arXiv:1802.02830, 2018.

[44] V. Zakharov, *Stability of periodic waves of finite amplitude on the surface of a deep fluid*, J. Appl. Mech. Technical Phys., 9 (1968), pp. 190–194.

[45] V. E. Zakharov and A. B. Shabat, *Exact theory of two-dimensional self-focusing and one-dimensional self-modulation of waves in nonlinear media*, Ž. Èksper. Teoret. Fiz., 61 (1971), pp. 118–134.